Table 2 Univariate and multivariate analysis in generation dataset

		Univariate analysis			Multivariate analysis		
	Patients (*n*)	HR	95% CI	*p* value	HR	95% CI	*p* value
Age (y)							
<65	124	(reference)	–	–			
≥65	137	0.88	0.60–1.28	0.49			
Gender							
Male	224	(reference)	–	–	(reference)	–	–
Female	37	0.39	0.18–0.83	0.015	0.34	0.16–0.75	0.008
PS							
0	75	(reference)	–	–	(reference)	–	–
1	186	2.38	1.45–3.91	0.001	0.75	0.41–1.37	0.35
Cancer site							
Lt	50	(reference)	–	–			
Ut	62	1.23	0.68–2.23	0.50			
Mt	149	1.33	0.81–2.17	0.26			
T stage (7th)							
1	80	(reference)	–	–	(reference)	–	–
2	17	2.76	1.04–7.36	0.042	2.21	0.75–6.56	0.15
3	105	5.17	2.77–9.65	<0.001	4.36	2.04–9.32	<0.001
4	59	6.61	3.43–12.76	<0.001	6.45	2.65–15.72	<0.001
N stage (7th)							
0	102	(reference)	–	–	(reference)	–	–
1	91	3.18	1.91–5.31	<0.001	1.87	1.07–3.28	0.029
2	60	4.52	2.65–7.70	<0.001	1.77	0.94–3.33	0.078
3	8	7.49	3.00–18.72	<0.001	2.78	0.96–8.05	0.059
M stage (7th)							
0	204	(reference)	–	–	(reference)	–	–
1	57	2.34	1.56–3.51	<0.001	1.08	0.68–1.70	0.75
Histological grade (7th)							
1	43	(reference)	–	–	(reference)	–	–
2	112	2.39	1.25–4.57	0.009	1.78	0.90–3.50	0.095
3	24	2.25	0.98–5.20	0.057	1.53	0.65–3.62	0.34
X	82	2.17	1.10–4.30	0.026	1.72	0.86–3.47	0.13
ND							
0	97	(reference)	–	–	(reference)	–	–
0–2.8	132	3.36	2.03–5.54	<0.001	1.83	1.03–3.25	0.041
>2.8	32	7.85	4.27–14.42	<0.001	3.48	1.62–7.46	0.001

Abbreviations: CI = confidence interval; HR = hazard ratio; Lt = lower thoracic portion; Mt = mid-thoracic portion; ND = the largest diameter of all the identified metastatic lymph nodes; PS = Eastern Cooperative Oncology Group performance status; Ut = upper thoracic portion.

was also considered as positive, even if lymph nodes were less than 5 mm in the short-axis diameter on CT.

Statistical analysis

All patient characteristics were considered categorical variables, with the exception of age, tumor length, and ND, which were treated as continuous data. Specific comparisons between groups were made using chi-square and Mann–Whitney tests. Overall survival was calculated from treatment initiation date to the time of death from any cause or to time of last follow-up. Survival curves were constructed using the Kaplan-Meier method, and log–rank tests were used to determine the statistical significance of differences. To evaluate the impact of each stage group on overall survival, univariate and multivariate Cox proportional hazards modeling was applied using the developmental database. Therefore, the measure of association in this study was the hazard ratio (HR) plus the 95% confidence interval (CI). Recursive partitioning analysis (RPA) was performed to determine the optimal cutoff point of ND and to develop the new staging classification using the developmental database (15). To develop the new staging, variables entered into the RPA were those that had attained statistical significance in the multivariate analysis. Subgroups having similar survival outcomes were combined. The newly formed stages were evaluated using the validation database. Statistical analyses were performed using the SPSS statistical software package version 11 (SPSS Inc., Chicago, IL) and R version 2.12.0 (R Project for Statistical Computing, Vienna, Austria). A p value less than 0.05 was considered statistically significant.

Results

Patient characteristics

The characteristics of the study patients are summarized in Table 1. NDs ranged from 0.5 to 7.0 cm, with a median ND of

1.7 cm in the developmental dataset, and ranged from 0.5 to 7.0 cm, with a median ND of 1.6 cm in the validation dataset. There was a higher proportion of patients receiving nedaplatin combined with 5-fluorouracil in the validation dataset ($p < 0.001$). The values for age, tumor length, T stage, N stage, histological grade, ND, and chemotherapy regimen were all significantly different between the developmental and validation datasets ($p < 0.05$). The median follow-up period was 60 months (range, 20–97 months), with 109 of the 261 patients dead at the time of analysis in the developmental dataset. The median follow-up period was 36 months (range, 12–64 months), with 66 of the 141 patients dead at the time of analysis in validation dataset.

Univariate and multivariate analysis

Figure 1 shows the survival curves according to the TNM 7th classification of each dataset. The 3-year survival rates of disease Stages I, II, III, and IV according to the TNM 7th classification were 89.9%, 70.1%, 38.7%, and 35.5%, respectively, in the developmental cohort (Fig. 1A). Kaplan-Meier analysis of overall survival revealed significant differences between Stages I and II ($p = 0.025$), and between II and III ($p = 0.0001$). Survival of Stage III patients almost completely overlapped the survival of Stage IV patients ($p = 0.58$). The overlap in survival of Stages III and IV was similar in the validation cohort (Fig. 1B).

Table 2 shows the univariate and multivariate analyses for each prognostic factor, including ND. According to RPA, ND stages were best when classified as ND0 (the absence of lymph node metastases), ND1 (<2.8 cm), and ND2 (≥2.8 cm). By univariate analysis, gender, performance status, TNM stages, histological grade, and ND were significant predictors of survival. By multivariate analysis, gender, T, N, and ND stage were independently and significantly associated with survival (all $p < 0.05$).

Development of new staging using RPA

To develop the new staging, RPA was performed on the developmental dataset. RPA that included gender, T, N, and ND stage as variables showed that ND was the initial discriminator of survival (Fig. 2). The significant RPA-derived splits were only the T and ND stages. For these five groups derived by RPA, the 3-year survival rates of groups I, II, III, IV, and V were 90.0%, 60.2%, 76.4%, 39.7%, and 21.5%, respectively. By the log–rank test, there were no significant differences in survival between groups I and III ($p = 0.07$) or between II and III ($p = 0.38$). Because survival of group II patients overlapped the survival of group III patients, groups II and III were combined. The resulting new staging system is shown in Table 3. There were significant differences between each stage (all $p < 0.05$ by log–rank test) (Fig. 3A). The 3-year survival rates of the new Stages I, II, III, and IV were 90.0%, 67.4%, 39.7%, and 21.5%, respectively (Fig. 3A).

External validation dataset

A total of 141 patients treated at Kansai Medical University were evaluated as the external validation dataset. Four new stages, determined from the RPA of the developmental dataset, were created. As shown in Fig. 3B, this new staging system resulted in well separated survival curves (all $p < 0.05$ by log–rank test). The

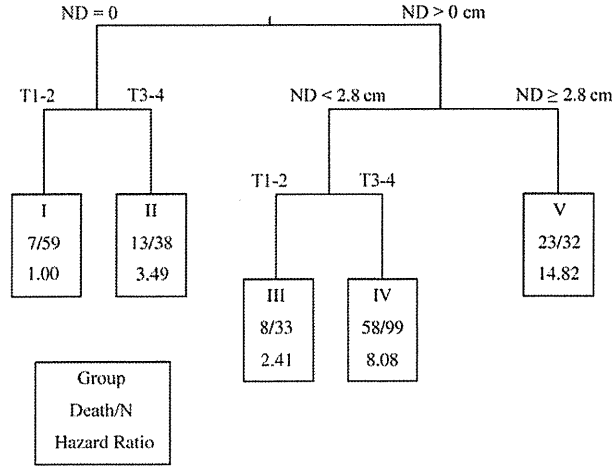

Fig. 2. Recursive partitioning analysis using gender, T, N, and ND stage as variables. In each terminal node, the upper row shows group number, the middle row shows the number of death and patients, and the low row shows the hazard ratio with reference to patients with Stage I.

3-year survival rates of the new Stages I, II, III, and IV were 90.2%, 53.2%, 22.6%, and 8.6%, respectively (Fig. 3B).

Discussion

Although neoadjuvant CRT followed by esophagectomy or definitive CRT have been standard therapies for resectable esophageal cancer (9, 10, 16–18), the 7th edition of the AJCC cancer staging system for esophageal cancer was based on pathologic data from patients treated by primary surgical resection alone (3). In the 7th edition, the new N factor, which was based on the number of positive regional lymph nodes and was redefined according to the locations of regional lymph nodes, is a major change from the 6th edition. Our previous report suggested that these staging criteria may be inappropriate for patients receiving CRT (4). Our results showed that the survival curve of Stage III patients almost overlapped the curve of Stage IV patients and that there were no

Table 3 New staging system

T classification	
T1	Tumor invasives lamina propria, muscularis mucosae, or submucosa
T2	Tumor invasives muscularis propria
T3	Tumor invasives adventitia
T4	Tumor invasives adjacent structures
N classification	
N0	No involved lymph nodes
N1	Metastasis in lymph node(s) less than 2.8 cm in greatest dimension
N2	Metastasis in a lymph node 2.8 cm or more in greatest dimension
New staging group	
I	T1–2N0
II	T1–2N1, T3–4N0
III	T3–4N1
IV	TanyN2

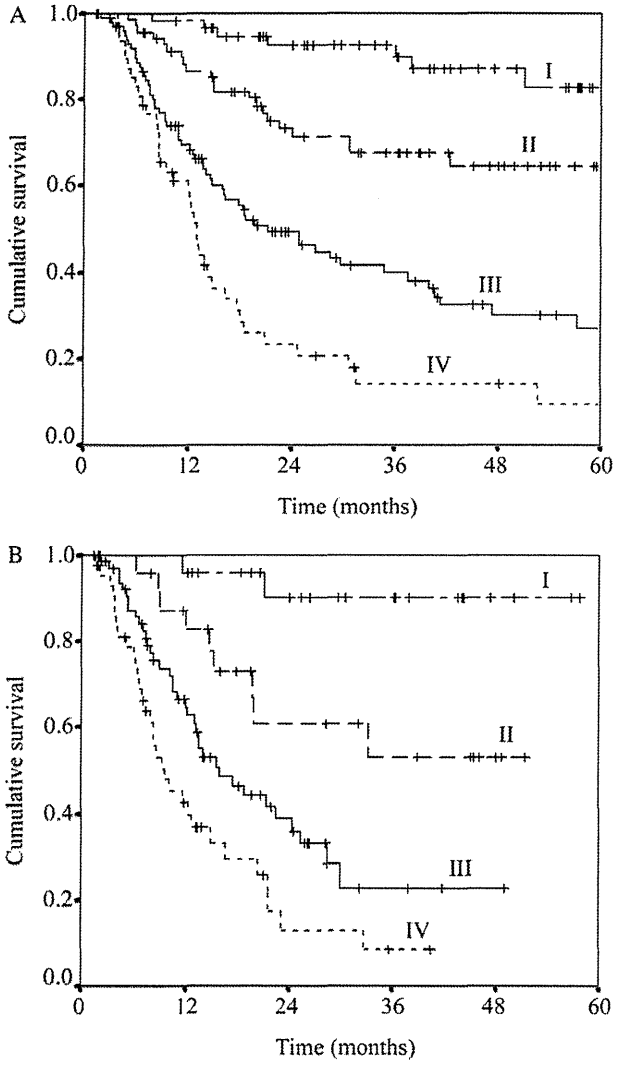

Fig. 3. Survival curves according to the new staging system of (A) the developmental dataset and (B) the validation dataset. The 3-year survival rates of the new Stage I, II, III, and IV were 90.0%, 67.4%, 39.7%, and 21.5%, respectively, in the developmental dataset. The 3-year survival rates of the new Stage I, II, III, and IV were 90.2%, 53.2%, 22.6%, and 8.6%, respectively, in the validation dataset.

significant prognostic differences between N1 and N3 diseases (4). Because the current staging system does not incorporate the size of involved lymph nodes, we performed two analyses: (*1*) the prognostic impact of ND was evaluated and (*2*) the new staging system was developed and validated for patients with esophageal squamous cell cancer who were treated with definitive CRT.

Our results showed that the size of lymph nodes, determined by ND, was the most significant factor for N assessments in patients with esophageal cancer undergoing definitive CRT. In previous studies, the number of lymph nodes, lymph node sizes, and metastatic to examined LN ratio were also significant prognostic factors for survival in esophageal cancer patients undergoing surgery alone (5, 6). Therefore, lymph node size may be a strong prognostic factor regardless of treatment modality.

RPA for patients in the developmental dataset referred with five terminal nodes. RPA indicated that the new N2 (ND $\geq$2.8 cm) was associated with the worst prognosis. By RPA, the 3-year survival rates of the patients staged with the new system were relatively similar in both the developmental and external validation cohorts. This new staging system resulted in good separation of the survival curves of both datasets. Thus, these results suggest ND is a more appropriate factor for incorporation in staging systems for patients with esophageal cancer undergoing definitive CRT than the current staging system. Incorporation of N staging, based on both the number of lymph nodes and ND, into the current staging system for esophageal cancer may improve clinical decision-making.

We recognize that our study has several limitations. First, only squamous cell carcinomas were evaluated, and all study patients were treated with the standard CRT for Japan (total radiation dose, 60 Gy) (9, 11). A second limitation is that this was a retrospective study using small number of patients. A third limitation is that several values in patient characteristics were significantly different between the developmental and validation datasets. Therefore, for validation, additional prospective, multicenter studies with large numbers of patients with adenocarcinoma or squamous cell carcinoma of the esophagus undergoing the current standard treatment, including neoadjuvant chemotherapy or CRT, are needed. Our results demonstrated that an ND of 2.8 cm is the most appropriate cutoff value, and more studies are needed to determine or validate the most appropriate cutoff value for ND.

In conclusion, our study demonstrated that lymph node size is a strong independent prognostic factor and that our new staging system, which incorporates lymph node size, as determined by ND, has good prognostic power and effectively discriminates patients with esophageal squamous cell cancer undergoing definitive CRT. We suggest that the revision of the current AJCC staging system for esophageal cancer should include N staging based on the size of involved lymph nodes.

References

1. Ajani JA, Barthel JS, Bekaii-Saab T, *et al.* Esophageal cancer. *J Natl Compr Canc Netw* 2008;6:818–849.
2. Edge SB, Byrd DR, Compton CC, *et al.* AJCC Cancer Staging Manual. 7th ed. New York: Springer; 2009.
3. Rice TW, Rusch VW, Ishwaran H, *et al.* Cancer of the esophagus and esophagogastric junction: Data-driven staging for the seventh edition of the American Joint Committee on Cancer/International Union Against Cancer Staging Manuals. *Cancer* 2010;116:3763–3773.
4. Nomura M, Shitara K, Kodaira T, *et al.* Prognostic impact of the 6th and 7th American Joint Committee on cancer TNM staging systems on esophageal cancer patients treated with chemoradiotherapy. *Int J Radiat Oncol Biol Phys* 2011 Feb 28 [Article in Press].
5. Komori T, Doki Y, Kabuto T, *et al.* Prognostic significance of the size of cancer nests in metastatic lymph nodes in human esophageal cancers. *J Surg Oncol* 2003;82:19–27.
6. Dhar DK, Hattori S, Tonomoto Y, *et al.* Appraisal of a revised lymph node classification system for esophageal squamous cell cancer. *Ann Thorac Surg* 2007;83:1265–1272.
7. International Commission of Radiation Units and Measurements. ICRU Report 50: Prescribing, recording, and reporting photon beam therapy. Bethesda, MD: International Commission on Radiation Units and Measurements; 1993.
8. International Commission of Radiation Units and Measurements. ICRU Report 62: Prescribing, recording, and reporting photon beam therapy (supplement to ICRU Report 50). Bethesda, MD: International Commission on Radiation Units and Measurements; 1999.

9. Ohtsu A, Boku N, Muro K, *et al.* Definitive chemoradiotherapy for T4 and/or M1 lymph node squamous cell carcinoma of the esophagus. *J Clin Oncol* 1999;17:2915–2921.
10. Minsky BD, Pajak TF, Ginsberg RJ, *et al.* INT 0123 (Radiation Therapy Oncology Group 94-05) phase III trial of combined-modality therapy for esophageal cancer: High-dose versus standard-dose radiation therapy. *J Clin Oncol* 2002;20:1167–1174.
11. Kato H, Sato A, Fukuda H, *et al.* A phase II trial of chemoradiotherapy for stage I esophageal squamous cell carcinoma: Japan Clinical Oncology Group Study (JCOG9708). *Jpn J Clin Oncol* 2009;39: 638–643.
12. Kodaira T, Fuwa N, Kamata M, *et al.* Single-institute phase I/II trial of alternating chemoradiotherapy with 5-FU and nedaplatin for esophageal carcinoma. *Anticancer Res* 2006;26:471–478.
13. Sumi H, Ohtsu A, Boku N, *et al.* A case of inoperable esophageal carcinoma with hepatic and nodal metastases which showed a long-term survival after chemoradiotherapy including nedaplatin. *Jpn J Clin Oncol* 2000;30:406–409.
14. Mizowaki T, Nishimura Y, Shimada Y, *et al.* Optimal size criteria of malignant lymph nodes in the treatment planning of radiotherapy for esophageal cancer: Evaluation by computed tomography and magnetic resonance imaging. *Int J Radiat Oncol Biol Phys* 1996;36: 1091–1098.
15. LeBlanc M, Crowley J. Relative risk trees for censored survival data. *Biometrics* 1992;48:411–425.
16. Stahl M, Walz MK, Stuschke M, *et al.* Phase III comparison of preoperative chemotherapy compared with chemoradiotherapy in patients with locally advanced adenocarcinoma of the esophagogastric junction. *J Clin Oncol* 2009;27:851–856.
17. Urschel JD, Vasan H. A meta-analysis of randomized controlled trials that compared neoadjuvant chemoradiation and surgery to surgery alone for resectable esophageal cancer. *Am J Surg* 2003;185: 538–543.
18. Herskovic A, Martz K, Al-Sarraf M, *et al.* Combined chemotherapy and radiotherapy compared with radiotherapy alone in patients with cancer of the esophagus. *N Engl J Med* 1992;326:1593–1598.

Treatment Outcome of Elderly Patients With Glioblastoma who Received Combination Therapy

Naoto Shikama, MD, Shigeru Sasaki, MD,† Atsunori Shinoda, MD,† and Keiichirou Koiwai, MD†*

Objectives: Large population-based registries in Western countries show that the treatment strategy for glioblastoma multiforme (GBM) in elderly patients is likely less intensive. The purpose of this study was to clarify the treatment outcome of elderly patients with GBM and to explore appropriate treatment strategies.

Methods: We analyzed records from 86 patients (median age, 59 y; range, 9 to 77 y) diagnosed and histologically confirmed to have GBM, between January 1991 and June 2006 at our institutions; 14 elderly patients (range, 71 to 77 y) and 72 younger patients (range, 9 to 70 y). Fifty-two patients underwent total or subtotal resection and 34 patients underwent partial resection or biopsy. The median radiation dose was 54 Gy and 79 patients (92%) received anticancer agents.

Results: Among the 51 patients in recursive partitioning analysis (RPA) classes 5 and 6, the median survival time of the 12 elderly and 39 younger patients were 10.5 months [95% confidence interval, 5.8-12.8] and 11.7 months (95% confidence interval, 9.3-13.0), respectively ($P = 0.32$). Multivariate analysis showed only RPA class as an independent prognostic factor for overall survival rate ($P = 0.009$), whereas age ($P = 0.85$), total radiation dose ($P = 0.052$), and treatment with anticancer agents ($P = 0.32$) were not.

Conclusions: After adjustment for RPA class, the treatment outcome of patients aged >70 years was equal to that of younger patients. Definitive treatment should not be withheld based on age alone.

Key Words: glioblastoma, prognostic factor, radiotherapy, elderly patients

(*Am J Clin Oncol* 2012;35:486–489)

Glioblastoma multiforme (GBM) is the most common glioma, occurring more often in patients in their 60s and 70s.[1,2] GBM is a rapidly progressive brain tumor, and the standard of care includes surgery, postoperative radiotherapy, and systemic chemotherapy.[1,3–6] In most clinical trials, the optimal treatment has been offered to only a selected subgroup of patients with GBM, such as those aged <70 years and with a good performance status (PS).[4,7] There is little information to define the standard of care for elderly patients with GBM.[6,8,9] Large population-based cancer registries in Western countries show that the treatment strategy for GBM in patients aged >70 years is likely to be less intensive and more palliative.[1,10] Data from the United States National Cancer Institute's Surveillance, Epidemiology, and End Results program showed that a total of 1412 patients with GBM (35%) received neither radiation nor chemotherapy, and patients who were elderly, unmarried, or had more comorbidities were less likely to receive radiotherapy and chemotherapy.[10,11] The cancer registry in Switzerland showed that although 56% of patients with GBM, aged 65 to 74 years, underwent surgery followed by radiotherapy, radiotherapy alone, or surgery alone, only 25% of the patients aged >75 years underwent surgery and/or radiotherapy.[12]

Some retrospective studies have shown that aggressive treatment is associated with prolonged survival in elderly patients with GBM. A study at the Memorial Sloan-Kettering Cancer Center demonstrated that, similar to studies in younger patients with GBM, age, PS, and extension of surgery were independent prognostic factors for treatment outcome of elderly patients, and emphasized that age alone should not disqualify patients from aggressive-combined treatment.[10] Results from the Cleveland Clinic showed that elderly patients aged >70 years with good PS, treated aggressively with maximal resection and definitive radiotherapy survived longer than those who received palliative radiotherapy and biopsy.[8] More prospective and retrospective studies are needed to establish the standard of care for elderly patients with GBM.

The purpose of this retrospective study was to clarify the treatment outcome of patients with GBM aged >70 years who received combination therapy, and to explore appropriate treatment strategies for elderly patients.

MATERIALS AND METHODS

We analyzed records from 86 patients (median age, 59 y; range, 9 to 77 y) who were diagnosed and histologically confirmed to have GBM between January 1991 and June 2006 at our institutions. Fourteen patients were aged >70 years (elderly patients; range, 71 to 77 y) and 72 patients were aged ≤70 years (younger patients; range, 9 to 70 y). Forty-six patients (53%) had good PS scores (0 to 1), whereas 40 (47%) had poor PS scores (2 to 4). The median preoperative tumor size was 4.5 cm (range, 1.4 to 8 cm; Table 1). Fifty-two patients (60%) underwent total or subtotal resection, and 34 (40%) underwent partial resection or biopsy. There was no difference in extension of surgery between elderly and younger patients ($P = 0.55$). O^6-methylguanine-DNA methyltransferase (MGMT) promoter methylation status was not assessed in all patients.

Radiotherapy started within 6 weeks postoperatively. As a basic procedure, clinical target volume was based on

From the *Department of Radiation Oncology, Saku Central Hospital; and †Department of Radiology, Shinshu University School of Medicine.

Supported by Health and Labor Sciences Research Grants (H21-018, H22-001), Grants-in-Aid for Cancer Research (20S-5), and a Grant-in-Aid for Scientific Research: Third term comprehensive control research for cancer (H22-043) from the Ministry of Health, Labor, and Welfare of Japan.

Presented in part at the 49th Annual Meeting of the American Society for Radiation Oncology, Los Angeles, SF, in October 2007.

The authors declare no conflicts of interest.

Reprints: Naoto Shikama, MD, Department of Radiology Oncology, Saku Central Hospital, 197 Usuda, Saku-City, Nagano, 384-0301 Japan. E-mail: nshikama0525@ gmail.com.

ISSN: 0277-3732/12/3505-0486
DOI: 10.1097/COC.0b013e31821a82ae

TABLE 1. Patient Characteristics

	Younger Patients (n = 72)		Elderly Patients (n = 14)	
	No. Patients (%)	Median (range)	No. Patients (%)	Median (range)
Age		57 y (9-70)		74 y (71-77)
Performance status				
0-1	44 (61%)		2 (14%)	
2-4	28 (39%)		12 (86%)	
RPA				
Class 3	14 (19%)		0 (0%)	
Class 4	19 (26%)		2 (14%)	
Class 5	25 (35%)		6 (43%)	
Class 6	14 (20%)		6 (43%)	
Tumor size		4.5 cm (1.4-8.0)		4.0 cm (3.0-6.5)
Surgery				
Total or subtotal resection	44 (61%)		8 (57%)	
Partial resection or biopsy	28 (39%)		6 (43%)	
Systemic therapy				
Chemotherapy	66 (92%)		9 (64%)	
Interferon-β	62 (86%)		8 (57%)	
External radiotherapy				
Fraction size		2 Gy (1.8-2)		2 Gy (2-3)
Total dose		54 Gy (42-66)		60 Gy (30-70)

RPA indicates recursive partitioning analysis proposed by the Radiation Therapy Oncology Group.

preoperative computed tomography (CT) and magnetic resonance imaging (MRI) studies, and included the enhanced tumor and peritumoral edema with 1.5 to 2 cm margins. The planning target volume (PTV) was based on clinical target volume with a 0.5 cm margin. If the PTV included critical organs, such as the brainstem, optic chiasm, optic nerve, or retina, PTV was reduced to a 1 to 1.5 cm margin of the preoperative gross tumor volume after a radiation dose of 50 Gy. A photon energy of 4 MV, 6 MV, or 10 MV was used. Treatment plans included lateral-opposed fields, wedged-pair fields, rotation techniques, or multiple-field techniques. Computer-aided treatment planning was performed after the late 1990s. The prescribed dose was calculated at the center of the radiation field or that of the PTV. A 74-year-old man with poor PS, who was grouped into class 6 by recursive partitioning analysis (RPA), was treated with 30 Gy in a fraction size of 3 Gy over 2 weeks. The remaining 85 patients were treated with 42 to 70 Gy in a fraction size of 1.8 to 2 Gy over 4 to 7 weeks. The median and mean radiation doses were 60 and 55 Gy (range, 30 to 70 Gy) in elderly patients, and 54 and 54 Gy (range: 42 to 66 Gy) in younger patients. There was no difference between the total radiation dose in elderly and younger patients ($P = 0.22$).

Seventy-nine patients (92%) received anticancer agents, including cytotoxic agents and/or interferon-β, during or after radiotherapy. Sixty-nine younger patients (96%) and 10 elderly patients (71%; $P=0.008$) received anticancer agents. Nitrosourea alone or nitrosourea-containing combination chemotherapy was administered to 75 patients, usually concomitant with radiotherapy and/or in a postradiotherapy adjuvant setting. Seventy patients received intravenous interferon-β at a dose of 3,000,000 IU daily during radiotherapy and weekly in a postradiotherapy adjuvant setting. As a basic procedure, patients received these anticancer agents until disease progression or development of severe adverse events. Temozolomide, an oral alkylating agent, was not used in the initial treatment of all patients. Temozolomide was approved for clinical use by the Ministry of Health, Labor, and Welfare of Japan in July 2006. Only a 59-year-old man, who was grouped into RPA class 4, was treated with temozolomide after local progression.

Overall survival time and progression-free survival (PFS) was measured from the date of treatment initiation. PFS was calculated using disease progression and death due to any cause such as events, and overall survival was calculated using death due to any cause such as an event. Disease progression was defined as an increase in tumor size compared with the initial tumor volume visualized on CT/MR images or the appearance of a new lesion separate from the initial tumor volume. Local progression was defined as a tumor size increase or new lesion in the surgical cavity seen on CT/MR images, and distant progression was defined as the appearance of new lesions separated from the initial tumors by at least 2 cm on CT/MR images. We used the Kaplan-Meier method to estimate survival distributions for each group and the log-rank test to compare survival distributions using a significance level of <0.05. The Mantel-Haenszel χ^2 test was used to compare patients and tumor characteristics at baseline. We carried out a multivariate analysis of prognostic factors using the Cox proportional hazards model. Statistical analysis was carried out using JMP version 5.1J (SAS Institute Inc.).

RESULTS

The median follow-up for all patients was 11.6 months (range, 1.4 to 105.8 mo). The median PFS and median survival time (MST) of all 86 patients were 5.8 months [95% confidence interval (CI), 4.7-7.4] and 12.8 months (95% CI, 10.8-14.9), respectively. One-year and 2-year overall survival rates of all patients were 53% and 16%, respectively. Thirteen patients (15%) showed disease progression at the end of radiotherapy. Twelve younger patients (17%) and 1 elderly patient (7%) showed local progression at the end of radiotherapy ($P=0.36$). The MST of the 35 patients in classes 3 and 4 was 16.9 months (95% CI, 14.2-22.7), and that of the 51 patients in classes 5 and 6 was 11.0 months (95% CI, 9.3-12.6; $P < 0.001$; Fig. 1).

Among the patients in classes 3 and 4, the MST of 2 elderly patients was 14.8 months (95% CI, 10.5-N/A), and that of 33 younger patients was 18.1 months (95% CI, 14.2-24.4;

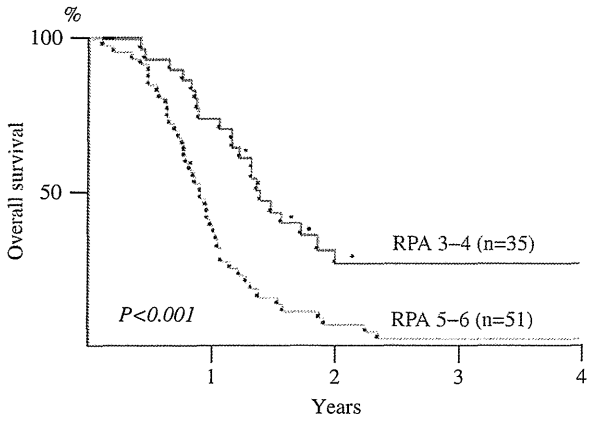

FIGURE 1. Comparison of overall survival rates based on recursive partitioning analysis (RPA) classes.

$P = 0.10$). Twelve elderly patients (86%) and 39 younger patients (54%) were grouped in RPA classes 5 and 6 (P=0.01). Among these patients, the MST of the 12 elderly patients was 10.5 months (95% CI, 5.8-12.8), and that of 39 younger patients was 11.7 months (95% CI, 9.3-13.0; P=0.32; Fig. 2). The 2-year overall survival rates of elderly and younger patients in classes 5 and 6 were 0% and 9%, respectively. The MST of the 20 middle-aged patients (61 to 70 y) in classes 5 and 6 was 8.8 months (95% CI, 6.7-12.0), and the 2-year overall survival rate was 0%. There was no difference between the MST of middle-aged patients and that of elderly patients (>70 y) ($P = 0.48$). The median PFS of elderly patients in classes 5 and 6 was 5.3 months (95% CI, 1.1-9.4), and that of younger patients was 5.8 months (95% CI, 3.2-7.2; $P = 0.74$). The median PFS of middle-aged patients in classes 5 and 6 was 3.6 months (95% CI, 1.7-7.2), and there was no difference between that of the middle-aged patients and that of elderly patients ($P = 0.70$). Among patients in classes 5 and 6, there was no difference between the extension of surgery and total radiation dose between elderly and younger patients ($P = 0.36$ and 0.69). However, younger patients received anticancer agents more frequently than elderly patients ($P = 0.03$).

We carried out a multivariate analysis including RPA class (3 to 4 vs. 5 to 6), age (60 to 70 y vs. >70 y), total radiation dose, and treatment with anticancer agents (yes vs. no). Only RPA class was an independent prognostic factor for overall survival rate ($P = 0.009$), whereas age ($P = 0.85$), total radiation dose (P=0.052), and treatment with anticancer agents ($P = 0.32$) were not. We also carried out a multivariate analysis including these prognostic factors for PFS, but found no independent prognostic factors (RPA classes, P=0.67; age, $P = 0.25$; total radiation dose, $P = 0.11$; anticancer agents, $P = 0.13$).

Sixty-five patients (75%) showed disease progression during the follow-up period: 54 patients (83%) had local progression, 8 (12%) had both local and distant progression, and 3 (5%) had only distant progression. Salvage therapies, including chemotherapy or best supportive care (BSC), were performed according to each physician's policy.

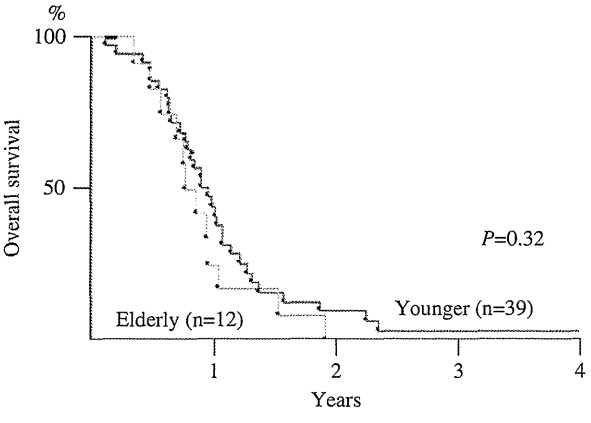

FIGURE 2. Overall survival rates of the 12 elderly patients and 39 younger patients in recursive partitioning analysis classes 5 and 6.

DISCUSSION

Data from the cancer registry in Switzerland demonstrated that 27% of patients with GBM aged 55 to 64 years, 44% of the patients aged 65 to 74 years, 75% of the patients aged >75 years received BSC alone without effective treatment.[12] The Surveillance, Epidemiology, and End Results-Medicare linked data demonstrated that increased age was associated with noneffective treatment and hence, worse prognosis.[13] Although these large population-based cancer registries demonstrate that an increase in age is associated with less intensive treatment, there is little information to define the standard of care for elderly patients with GBM.[9] In particular, there are no prospective randomized studies that evaluate the effectiveness and safety of combination therapy, including postoperative radiotherapy and chemotherapy, for patients aged $\geq$ 70 years.

Adjuvant systemic chemotherapy after surgery prolongs survival in patients with GBM.[6,14] A meta-analysis of 12 randomized controlled trials, including more than 3000 patients, compared postoperative radiotherapy alone with postoperative radiotherapy and chemotherapy, and demonstrated that the addition of chemotherapy decreased the risk of death by 15% (hazard ratio, 0.85; 95% CI, 0.78-0.91).[5] The European Organisation for Research and Treatment of Cancer/the National Cancer Institute of Canada Intergroup conducted a randomized clinical trial for patients aged 18 to 70 years with newly diagnosed GBM, and reported that the 2-year survival rate was 26% for the temozolomide and radiotherapy group compared with only 10% for the radiation only group.[4] This trial demonstrated the clinical benefit of temozolomide in patients with GBM, but subset analysis showed that the benefit was not statistically significant in patients undergoing diagnostic biopsy only or those with poor PS.[4,15] The 5-year analysis of this trial demonstrated that patients aged 60 to 70 years benefited from combined therapy (hazard ratio for overall survival, 0.7; range, 0.5 to 0.97).[16] Grant et al[17] retrospectively analyzed 148 patients with malignant gliomas or recurrent astrocytomas who received nitrosourea-based chemotherapy, and reported that age was strongly predictive of the likelihood of responding to chemotherapy, time to progression, and survival, and patients aged $\geq$ 60 years had a lower chance of benefiting from chemotherapy. On the other hand, Combs et al[18] conducted a retrospective study including 43 patients aged $\geq$ 65 years (range, 65 to 76 y) who received postoperative radiotherapy and chemotherapy, and reported that radiochemotherapy was safe and effective in this population. Prospective studies are required to clarify the benefit of chemotherapy for elderly patients with GBM.

The Medical Research Council conducted a randomized trial comparing 45 Gy in 20 fractions over 4 weeks with 60 Gy

in 30 fractions over 6 weeks for patients aged 18 to 70 years with grade 3 or 4 malignant glioma, and reported that the 60 Gy course produced a modest lengthening of PFS and overall survival.[19] Keime-Guibert et al[6] conducted a randomized trial that compared BSC only with radiotherapy (50 Gy in daily fractions of 1.8 Gy over 5 wk) in patients with GBM aged ≥ 70 years. Radiotherapy improved MST from 16.9 weeks to 29.1 weeks, and the hazard ratio for death in the radiotherapy group was 0.47 (95% CI, 0.29-0.76; P=0.002). Roa et al[20] conducted a prospective randomized trial that compared standard radiation therapy (60 Gy in 30 fractions over 6 wk) and a short course of radiotherapy (40 Gy in 15 fractions over 3 wk) in patients aged ≥ 60 years. There was no difference in survival between the 2 groups, and short-course radiotherapy led to a decrease in posttreatment corticosteroid dosage. Although radiotherapy has been effective and safe in elderly patients, it is unclear whether a total dose of 60 Gy represents the standard dose for these patients.[6,19] A limitation of this study is that the median radiation dose for younger patients was <60 Gy. However, there was no statistical difference between the radiation dose in elderly, middle-aged, and younger patients and multivariate analysis showed that total radiation dose was not associated with overall survival. This study is also limited due to the lack of evaluation of MGMT methylation status, quality of life, and long-term neurotoxicity.

Although age is an important factor for predicting survival of patients with GBM, there is a room for discussion as to whether less intensive therapy is suitable for the majority of elderly patients.[8,9] RPA proposed by the Radiation Therapy Oncology Group has been a useful tool for predicting the prognosis of patients with malignant glioma.[21] RPA includes age, histology, mental status, PS, and the extent of surgical excision. The median survival time was 4.7 to 58.6 months for the 12 subgroups resulting from this analysis. This study showed that the MST of the 35 patients in classes 3 and 4 was superior to that of 51 patients in classes 5 and 6 (P < 0.001). However, a limitation of the RPA classification is that it requires the extent of surgical excision, which cannot be assessed before treatment, and this prognostic system is not used for the initial pretreatment decision-making process. The Organisation for Research and Treatment of Cancer/the National Cancer Institute of Canada Clinical Trials Group developed nomograms for predicting survival in patients with GBM. The nomograms include methylated MGMT promoter status, age, PS, extension of surgical excision, and Mini-Mental State Examination score.[7] Patients with GBM with a methylated MGMT promoter benefit from temozolomide and have a good prognosis.[22] This additional molecular information may be useful for estimating the treatment outcome of patients with GBM, and other molecular characteristics and predictive markers may facilitate individually tailored therapy.

In this study, the majority of elderly patients were grouped in RPA classes 5 and 6. However, an analysis adjusting for RPA classification showed that the treatment outcome of patients aged >70 years in classes 5 and 6 and that of younger patients in classes 5 and 6 was likely to be equal. Treatment decision-making should be performed in the same manner in elderly patients as for younger patients, and definitive treatment should not be withheld based on age alone.

ACKNOWLEDGMENTS

The authors are grateful to Dr T. Tada (Department of Neurosurgery, Shinshu University, School of Medicine) for clinical support and to Mrs Y. Asazawa and Mrs M. Kikuhara for their technical assistance.

REFERENCES

1. DeAngelis LM. Brain tumors. *N Engl J Med.* 2001;344:114–123.
2. Surawicz TS, McCarthy BJ, Kupelian V, et al. Descriptive epidemiology of primary brain and CNS tumors: results from the Central Brain Tumor Registry of the United States, 1990-1994. *Neuro Oncol.* 1999;1:14–25.
3. Reardon DA, Rich JN, Friedman HS, et al. Recent advances in the treatment of malignant astrocytoma. *J Clin Oncol.* 2006;24:1253–1265.
4. Stupp R, Mason WP, van den Bent MJ, et al. Radiotherapy plus concomitant and adjuvant temozolomide for glioblastoma. *N Engl J Med.* 2005;352:987–996.
5. Stewart LA. Chemotherapy in adult high-grade glioma: a systematic review and meta-analysis of individual patient data from 12 randomised trials. *Lancet.* 2002;359:1011–1018.
6. Keime-Guibert F, Chinot O, Taillandier L, et al. Radiotherapy for glioblastoma in the elderly. *N Engl J Med.* 2007;356:1527–1535.
7. Gorlia T, van den Bent MJ, Hegi ME, et al. Nomograms for predicting survival of patients with newly diagnosed glioblastoma: prognostic factor analysis of EORTC and NCIC trial 26981-22981/CE.3. *Lancet Oncol.* 2008;9:29–38.
8. Mohan DS, Suh JH, Phan JL, et al. Outcome in elderly patients undergoing definitive surgery and radiation therapy for supratentorial glioblastoma multiforme at a tertiary care institution. *Int J Radiat Oncol Biol Phys.* 1998;42:981–987.
9. Hutterer M. Elderly patients with glioblastoma multiforme—an underestimated subpopulation?. *Neuroepidemiology.* 2009;33:23–24.
10. Iwamoto FM, Cooper AR, Reiner AS, et al. Glioblastoma in the elderly: the Memorial Sloan-Kettering Cancer Center Experience (1997–2007). *Cancer.* 2009;115:3758–3766.
11. Iwamoto FM, Reiner AS, Panageas KS, et al. Patterns of care in elderly glioblastoma patients. *Ann Neurol.* 2008;64:628–634.
12. Kita D, Ciernik IF, Vaccarella S, et al. Age as a predictive factor in glioblastomas: population-based study. *Neuroepidemiology.* 2009;33:17–22.
13. Barnholtz-Sloan JS, Williams VL, Maldonado JL, et al. Patterns of care and outcomes among elderly individuals with primary malignant astrocytoma. *J Neurosurg.* 2008;108:642–648.
14. Fine HA, Dear KB, Loeffler JS, et al. Meta-analysis of radiation therapy with and without adjuvant chemotherapy for malignant gliomas in adults. *Cancer.* 1993;71:2585–2597.
15. Stupp R, Hegi ME, van den Bent MJ, et al. Changing paradigms—an update on the multidisciplinary management of malignant glioma. *Oncologist.* 2006;11:165–180.
16. Stupp R, Hegi ME, Mason WP, et al. Effects of radiotherapy with concomitant and adjuvant temozolomide versus radiotherapy alone on survival in glioblastoma in a randomised phase III study: 5-year analysis of the EORTC-NCIC trial. *Lancet Oncol.* 2009;10:459–466.
17. Grant R, Liang BC, Page MA, et al. Age influences chemotherapy response in astrocytomas. *Neurology.* 1995;45:929–933.
18. Combs SE, Wagner J, Bischof M, et al. Postoperative treatment of primary glioblastoma multiforme with radiation and concomitant temozolomide in elderly patients. *Int J Radiat Oncol Biol Phys.* 2008;70:987–992.
19. Bleehen NM, Stenning SP. A Medical Research Council trial of two radiotherapy doses in the treatment of grades 3 and 4 astrocytoma. The Medical Research Council Brain Tumour Working Party. *Br J Cancer.* 1991;64:769–774.
20. Roa W, Brasher PM, Bauman G, et al. Abbreviated course of radiation therapy in older patients with glioblastoma multiforme: a prospective randomized clinical trial. *J Clin Oncol.* 2004;22:1583–1588.
21. Curran WJ Jr, Scott CB, Horton J, et al. Recursive partitioning analysis of prognostic factors in three Radiation Therapy Oncology Group malignant glioma trials. *J Natl Cancer Inst.* 1993;85:704–710.
22. Hegi ME, Diserens AC, Gorlia T, et al. MGMT gene silencing and benefit from temozolomide in glioblastoma. *N Engl J Med.* 2005;352:997–1003.

Radiotherapy and Oncology 104 (2012) 390–394

Contents lists available at SciVerse ScienceDirect

Radiotherapy and Oncology

journal homepage: www.thegreenjournal.com

Prostate radiotherapy

Large prostate motion produced by anal contraction

Hiroshi Onishi [a,*], Kengo Kuriyama [a], Takafumi Komiyama [a], Kan Marino [a], Masayuki Araya [a], Ryo Saito [a], Shinichi Aoki [a], Yoshiyasu Maehata [a], Licht Tominaga [a], Naoki Sano [a], Mitsuhiko Oguri [a], Kojiro Onohara [a], Iori Watanabe [a], Tsuyota Koshiishi [a], Kazuhiko Ogawa [b], Tsutomu Araki [a]

[a] University of Yamanashi; and [b] University of the Ryukyus, Okinawa, Japan

ARTICLE INFO

Article history:
Received 28 July 2010
Received in revised form 4 December 2011
Accepted 29 April 2012
Available online 5 June 2012

Keywords:
Prostate
Radiotherapy
Intrafractional motion
Anal contraction
Anal levator muscle

ABSTRACT

Background and purpose: The aim of this study was to define the effects of voluntary anal contraction on prostate motion in an experimental setting.
Materials and methods: Thirty-eight patients (median age, 76 years) with prostate cancer underwent thin-slice computed tomography (CT) in the vicinity of the prostate before and after active anal contraction. Three-dimensional displacement of the pelvis and prostate was measured.
Results: Mean (±standard deviation, SD) overall displacement of the prostate due to anal contraction was 0.3 ± 1.4 mm to the right, 9.3 ± 7.8 mm to the anterior, and 5 ± 4 mm to the cranial direction. Mean displacement of the pelvis was 0.5 ± 1.8 mm to the right, 4.1 ± 7.1 mm to the anterior, and 1 ± 3 mm to the cranial direction. Mean displacement of the prostate relative to the pelvis was 0.1 ± 1.1 mm to the left, 5.2 ± 3.3 mm to the anterior, and 4 ± 4 mm to the cranial direction.
Conclusions: Voluntary anal contraction within an experimental setting induces large prostate and bone motion, mainly in the anterior and cranial directions. The frequency and magnitude of actual anal contractions during radiotherapy for prostate cancer need to be determined.

Targeting the prostate with external beam radiotherapy requires consideration of the positioning uncertainties involved in delivering the intended dose to the target. The International Commission on Radiation Units and Measurements (ICRU) has provided standardized target and uncertainty definitions, which are detailed in ICRU reports 50 and 62 [1,2]. Inadequate margins result in underdosing of the target, whereas unnecessarily large margins are associated with the increased morbidity of nearby critical structures. Dose escalation relies on the minimization of margins during treatment planning to ensure an acceptable toxicity profile. In the case of localized prostate cancer, late rectal toxicity is considered to be the dose-limiting factor in prostate radiotherapy [3–5]. Correction of interfractional movement improves radiation treatment accuracy if geometrical changes are within certain limits [6,7]. More precise targeting (localization) of the prostate permits the use of smaller margins, which should result in reduced treatment toxicity [8,9] and/or allow for increased dose delivery [10] without changing the accompanying toxicity profile.

The treatment regimen is usually based on the contouring of a single planning computed tomography (CT) scan. However, organ mobility leads to discrepancies in the position of the target volume at the time of the scan vs. during actual treatment. Accurate interfractional patient and prostate repositioning before prostate radiotherapy has become possible in the era of image-guided radiotherapy (IGRT) [11], with several in-room systems now available, such as stereotactic ultrasound [12,13], beacon responders [14], and kilovolt or megavolt cone- or fan-beam CT-based methods [15–17]. However, intrafractional prostate motion remains a difficult problem [18–33]. The prostate, which has been called the "dancing organ", must be considered as an inter- and intrafractionally moving target due to constant changes in rectal filling [20–29], although unexplained large intrafractional prostate motion despite a lack of changes in rectal or bladder volume has been observed. We suggest that there is a relationship between the motion of anal contraction and prostate motion. During the radiotherapy of prostate cancer, voluntary or involuntary motion of anal contractions may be triggered to repress gas or loose stool, either of which may accumulate in response to radiation-induced diarrhea or the activation of bowel motion. The present study therefore examined potential relationships between the experimentally voluntary action of anal contraction and internal prostate motion.

Materials

Institutional review board approval was received for this study, and all patients included in the study provided written informed consent prior to participation.

* Corresponding author. Address: Department of Radiology, School of Medicine, University of Yamanashi, 1110 Shimokato, Chuo City, Yamanashi 409-3898, Japan.
E-mail address: honishi@yamanashi.ac.jp (H. Onishi).

0167-8140/$ - see front matter © 2012 Elsevier Ireland Ltd. All rights reserved.
http://dx.doi.org/10.1016/j.radonc.2012.04.005

From April 2007 to March 2009, all patients (median age, 76 years; range, 66–85 years) with localized prostate cancer who were scheduled to receive radiotherapy and whose prostates showed focal calcification were selected as subjects. Focal calcifications in the prostate were used to measure prostate motion.

Methods

The 38 patients enrolled in the study were informed as to its concept, methodology, and rationale, and subsequently provided written informed consent. The patients were then given instruction as to how to actively contract the anus. Specifically, they were asked to contract the anus as if they were repressing the passage of bowel gas or loose stool. After patients indicated that they fully understood how to voluntarily contract the anus, CT (Hi-Speed DX/I; GE Yokogawa Medical Systems, Tokyo, Japan) was performed before and after active anal contraction to obtain images of 2-mm thickness in the vicinity of the prostate. Patients were requested to maintain the anal contraction during the entire scan, which lasted approximately 5 s. Measured points were fixed at a distinct focal calcification in each prostate and at the upper tip of the pubic symphysis. Differences in the measurement points between the two sets of CT scans, i.e., before and after the voluntary anal contraction, were calculated by visual comparison on the same CT monitor along three axes: x, left–right; y, antero-posterior; and z, cranio-caudal. The cranio-caudal difference was calculated as the difference in CT table position of slices in which the fixed measurement point was displayed, in most cases using a unit of 2 mm. However, if the measurement point was considered to be present between two consecutive CT slices, the position was calculated using units of 1 mm. Translational displacements in the left–right and antero-posterior directions were determined by subtracting the coordinates of the tumor center in one CT series from those in the other CT series. Mean values (±standard deviation, SD) were calculated for all displacements in each direction. The length of the displacement vector was calculated using the formula: $v = \sqrt{[(\text{difference along } x)2 + (\text{difference along } y)2 + (\text{difference along } z)2]}$. Overall prostate motion was defined as the crude displacement of the focal calcification in the prostate. Pelvic motion was defined as displacement of the upper tip of the pubic symphysis, and internal prostate motion as the displacement of the prostate relative to the pelvis.

Results

Maximum, mean, SD, and overall vector length of the prostate and the pelvic displacements with voluntary anal contraction are shown in Table 1.

Overall prostate motion due to anal contraction

The mean overall motion of the prostate (i.e., of the focal calcification in the prostate) due to anal contraction was 0.3 ± 1.4 mm to the right, 9.3 ± 7.8 mm to the anterior, and 5 ± 4 mm to the cranial direction. The mean overall displacement vector length of the prostate was 10.5 ± 8.2 mm.

Motion of the pelvis due to anal contraction

Mean pelvic motion (i.e., of the upper tip of the pubic symphysis) due to anal contraction was 0.5 ± 1.8 mm to the right, 4.1 ± 7.1 mm to the anterior, and 1 ± 3 mm to the cranial direction. The mean overall displacement vector length of the pelvis was 4.3 ± 7.1 mm.

Internal prostate motion due to anal contraction

The mean internal prostate motion relative to the pelvis due to anal contraction was 0.1 ± 1.1 mm to the left, 5.2 ± 3.3 mm to the anterior, and 4 ± 4 mm to the cranial direction. The mean overall displacement vector length of the pelvis was 6.6 ± 4.5 mm.

Case examples

An example obtained from a patient with large motion in the internal prostate position due to the voluntary anal contraction is shown in Fig. 1. Rectal and bladder volumes in this case were almost unchanged after anal contraction.

An example from another patient, in whom the voluntary anal contraction caused large motions in the pelvis and internal prostate position, is shown in Fig. 2.

Discussion

The anal levator muscle is one of a pair of muscles of the pelvic diaphragm that stretches across the bottom of the pelvic cavity like a hammock, supporting the pelvic organs. Among the components of the anal levator muscle, a portion of the anterior pubococcygeus muscle is called the levator muscle of the prostate because it inserts into both the prostate and the tendinous center of the perineum. Therefore, voluntary or involuntary anal contraction arouses internal motion of the prostate mainly in an anterior–cranial direction. The relationship between contraction of the anal levator muscle and prostate motion is illustrated in Fig. 3.

The magnitude of intrafractional motion of the prostate during radiotherapy has been demonstrated in numerous reports [18,19,26,30–33], as shown in Supplementary material, and has

Table 1
Analysis of pelvic and internal prostate motion due to anal contraction.

$n = 38$	Direction	Max[a] (mm)	Mean (mm)	SD[b] (mm)
Overall motion	R–L	R 2.4, L 3.9	R 0.3	1.4
	A–P	A 32.2, P 0.5	A 9.3	7.8
	Cr–Ca	Cr 16, Ca 2	Cr 5	4
	Vector length	34.4	10.5	8.2
Motion of pelvis	R–L	R 2.9, L 4.9	R 0.5	1.8
	A–P	A 27.3, P 1.4	A 4.1	7.1
	Cr–Ca	Cr 12, Ca 2	Cr 1	3
	Vector length	28.5	4.3	7.1
Internal prostate motion (relative to pelvis)	R–L	R 3.4, L 2.0	L 0.1	1.1
	A–P	A 12.2, P 1.0	A 5.2	3.3
	Cr–Ca	Cr 16, Ca 2	Cr 4	4
	Vector length	19.4	6.6	4.5

[a] Movement in each direction. R, right; L, left; A, anterior; P, posterior; Cr, cranial; Ca, caudal.
[b] Movement from the original position, before anal contraction, was calculated as an absolute value.

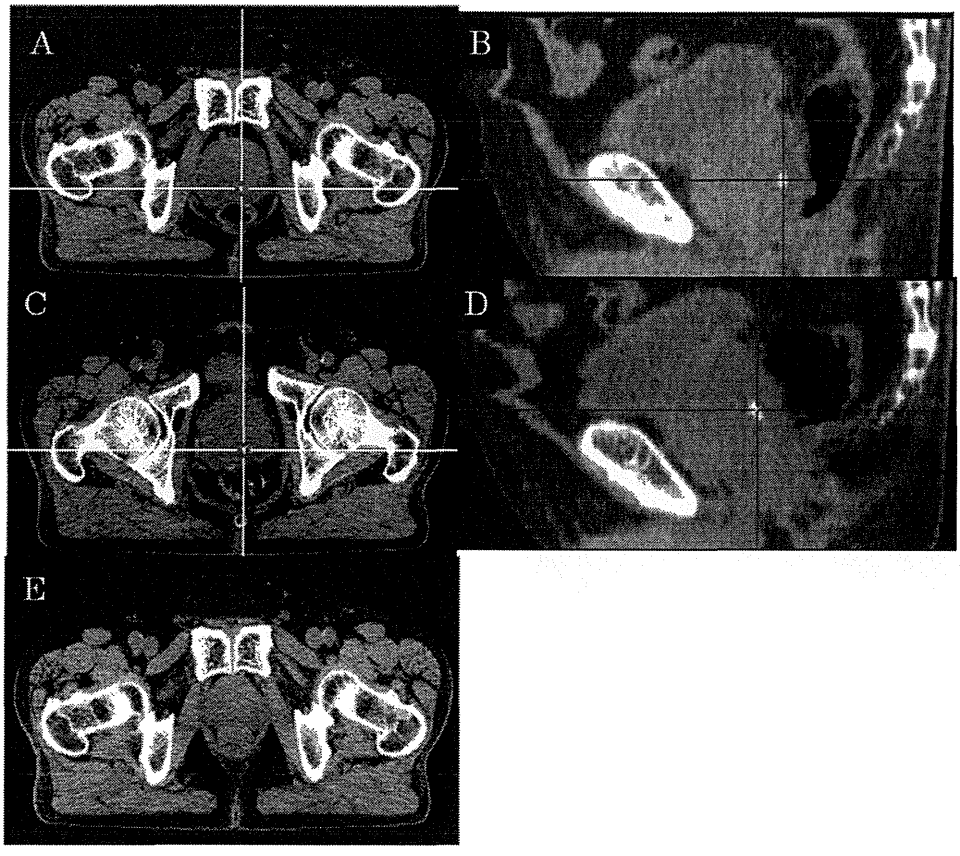

Fig. 1. Large motion in the internal prostate position due to anal contraction as determined (A: axial, B: sagittal) before and (C: axial, D: sagittal) after anal contraction. The cross-lines indicate the focal calcification in the prostate used to measure motion. (E) The designated slice is the same as in (A) based on an identical bone section. The prostate moved internally 10.9 and 16.0 mm in the anterior and cranial directions, respectively. Rectal and bladder volumes were unchanged after anal contraction. The rectum also moved anteriorly (E).

mostly been considered to result from volumetric changes to the rectum or bladder. Ten Haken et al. reported that a comparison of CT-based treatment plans to simulator films taken with the rectum and bladder opacified yielded indirect evidence of movement of the prostate gland by $\geqslant$0.5 cm in 31 of 50 consecutive patients [21]. Ghilezan et al. reported that the most significant predictor for intrafraction prostate motion is the status of rectal filling [25]. Both et al. reported that daily insertion of an endorectal balloon could consistently stabilize the prostate, preventing clinically significant displacement (>5 mm) [23]. To the best of our knowledge, this represents the first report on prostate internal motion related to anal contraction in patients with prostate cancer in an experimental setting. The effect of anal contractions on prostate motion in a healthy man was also examined using MRI. Mikuma et al. reported that the prostate and bladder base moved anterocranially by 0–12 mm [34] in an experimental setting. On sagittal images, anal contraction pulled the prostate and rectum closer to the pubic bone. Contraction of the levator ani muscle accompanied anal contraction, and resulted in two dynamic changes in configuration of the pelvic floor: (1) up-forward movement of the bladder and prostate and (2) forward movement of the rectum. Similar findings were reported by Christensen et al. using MRI [35].

In the present study, anal contraction provided evidential support for the anterior–cranial movement of the prostate during the voluntary action in the patients with prostate cancer in an experimental setting. In some patients, the pelvis simultaneously moved mainly forward with prostate motion, most likely due to contraction of the gluteal muscles, which, in turn, was caused by the strong anal contraction. Therefore, fixing the pelvis with a shell may be important in patients with diarrhea or rectal gas accumulation produced by radiation-induced activation of bowel motion. However, it is noteworthy that even with shell fixation, large internal intrafractional motion of the prostate, which is sometimes rotational as shown in the case example in Fig. 2, can occur following anal contraction in an experimental setting. Moreover, it is also important to know that the prostate may be not only displaced but also deformed by anal contraction, although this aspect was not addressed herein.

This study has three limitations. First, it is uncertain whether the participants properly understood the intent of the study and the importance of properly performing anal contraction. Second, if, as is likely the case, contraction induces rotations and deformations in addition to translations of the prostate gland, such rotation is better studied three dimensionally. Third, this study is based on an experimentally voluntary anal contraction. The actual frequency and size of the involuntary anal contraction that typically occurs in prostate cancer patients undergoing radiotherapy are unknown. These issues should be further investigated to demonstrate the relevance of anal contraction to radiotherapy planning and results.

If prostate motion derived from anal contraction as described in this study occurs during actual treatment, it might be lessened by employing proper measures against diarrhea and rectal gas accumulation caused by pelvic irradiation, such as by administering either loperamide or scopolamine. Nichol et al. reported that an

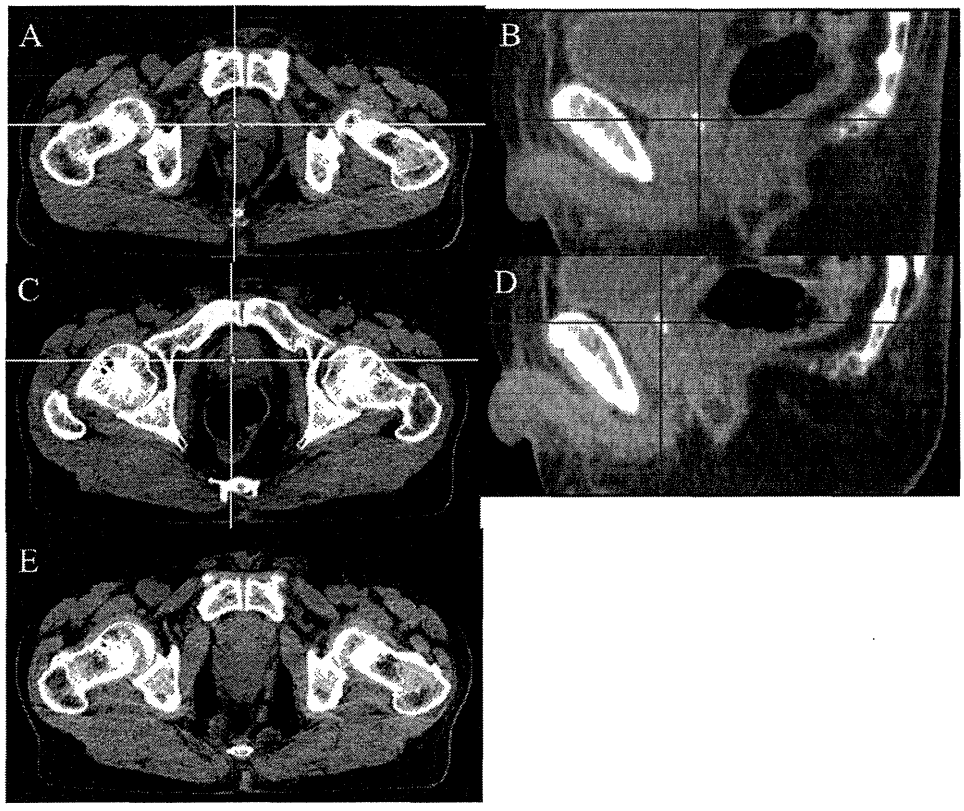

Fig. 2. Large motions in both the pelvis and internal prostate position due to anal contraction as determined (A: axial, B: sagittal) before and (C: axial, D: sagittal) after anal contraction. The cross-lines indicate the focal calcification in the prostate used to measure motion. (E) The designated slice is the same as in (A) based on an identical bone section. Contraction of the gluteal muscle together with the anal contraction resulted in movement of the pelvis 10.7 and 4.0 mm in the anterior and cranial directions, respectively. Additionally, the prostate moved internally 10.5 and 12.0 mm in the anterior and cranial directions, respectively. The rectum moved anteriorly and rectal gas moved away (D). In this case, the prostate simultaneously showed rotational motion.

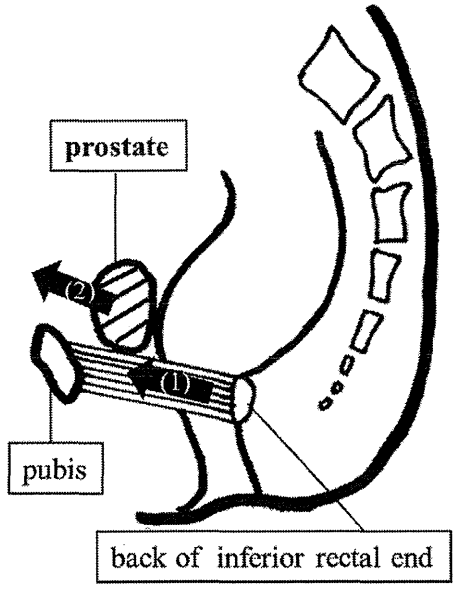

Fig. 3. The relationship between contraction of the anal levator muscle and prostate motion. Anal contraction [1] causes the prostate to move, mainly in the anterior and cranial directions [2].

antiflatulent diet and milk of magnesia did not significantly reduce intrafractional prostate motion [24]. This may be because the effect of treatment for voiding rectal subjects simultaneously induced bowel motion including anal contractions. Padhani et al. reported that the incidence of rectal movements correlated with receiving bowel relaxants, and the magnitude of rectal movements correlated well with degree of prostate movement [22]. Routine patient instruction to avoid anal contraction may be another simple measure. Madsen et al. commented that it may be advisable to allow for a short settling-in period before actually delivering treatment [19].

Conclusions

The prostate moves largely in an anterior–cranial direction on voluntary anal contraction in an experimental setting even if pelvic motion is controlled. But the real impact of non-voluntary random anal contraction on prostate movement and the relevance of it in relation to the rectal filling need to be determined in future within an appropriate clinical setting.

Conflict of interest statement

None of the authors have a conflict of interest in this work.

Appendix A. Supplementary data

Supplementary data associated with this article can be found, in the online version, at http://dx.doi.org/10.1016/j.radonc.2012.04.005.

References

[1] International Commission on Radiation Units and Measurements. ICRU report 50: prescribing, recording, and reporting photon beam therapy. Bethesda, MD: International Commission on Radiation Units and Measurements; 1993.

[2] International Commission on Radiation Units and Measurements. ICRU report 62: prescribing, recording and reporting photon beam therapy (supplement to ICRU report 50). Bethesda, MD: International Commission on Radiation Units and Measurements; 1999.

[3] Brenner DJ. Fractionation and late rectal toxicity. Int J Radiat Oncol Biol Phys 2004;60:1013–5.

[4] Jackson A, Skwarchuk MW, Zelefsky MJ, et al. Late rectal bleeding after conformal radiotherapy of prostate cancer. II. Volume effects and dose–volume histograms. Int J Radiat Oncol Biol Phys 2001;49:685–98.

[5] Schultheiss TE, Lee WR, Hunt MA, Hanlon AL, Peter RS, Hanks GE. Late GI and GU complications in the treatment of prostate cancer. Int J Radiat Oncol Biol Phys 1997;37:3–11.

[6] Dobler B, Mai S, Ross C, et al. Evaluation of possible prostate displacement induced by pressure applied during transabdominal ultrasound image acquisition. Strahlenther Onkol 2006;182:240–6.

[7] Fiorino C, Foppiano F, Franzone P, et al. Rectal and bladder motion during conformal radiotherapy after radical prostatectomy. Radiother Oncol 2005;74:187–95.

[8] Guckenberger M, Pohl F, Baier K, Meyer J, Vordermark D, Flentje M. Adverse effect of a distended rectum in intensity-modulated radiotherapy (IMRT) treatment of prostate cancer. Radiother Oncol 2006;79:59–64.

[9] van Lin EN, Hoffmann AL, van Kollenburg P, Leer JW, Visser AG. Rectal wall sparing effect of three different endorectal balloons in 3D conformal and IMRT prostate radiotherapy. Int J Radiat Oncol Biol Phys 2005;63:565–76.

[10] de Crevoisier R, Tucker SL, Dong L, et al. Increased risk of biochemical and local failure in patients with distended rectum on the planning CT for prostate cancer radiotherapy. Int J Radiat Oncol Biol Phys 2005;62:965–73.

[11] Fuss M, Boda-Heggemann J, Papanikolau N, Salter BJ. Image guidance for stereotactic body radiation therapy. Med Dosim 2007;32:102–10.

[12] Boda-Heggemann J, Kohler FM, Kupper B, et al. Accuracy of ultrasound-based (BAT) prostate repositioning: a three-dimensional on-line fiducial-based assessment with cone-beam computed tomography. Int J Radiat Oncol Biol Phys 2008;70:1247–55.

[13] Fuss M, Cavanaugh SX, Fuss C, Cheek DA, Salter BJ. Daily stereotactic ultrasound prostate targeting: inter-user variability. Technol Cancer Res Treat 2003;2:161–70.

[14] Willoughby TR, Kupelian PA, Pouliot J, et al. Target localization and real-time tracking using the Calypso 4D localization system in patients with localized prostate cancer. Int J Radiat Oncol Biol Phys 2006;65:528–34.

[15] de Crevoisier R, Kuban D, Lefkopoulos D. Image-guided radiotherapy by in-room CT-linear accelerator combination. Cancer Radiother 2006;10:245–51.

[16] Jaffray DA. Kilovoltage volumetric imaging in the treatment room. Front Radiat Ther Oncol 2007;40:116–31.

[17] Pouliot J. Megavoltage imaging, megavoltage cone beam CT and dose-guided radiation therapy. Front Radiat Ther Oncol 2007;40:132–42.

[18] Budiharto T, Slagmolen P, Haustermans K, et al. Intrafractional prostate motion during online image guided intensity-modulated radiotherapy for prostate cancer. Radiother Oncol 2011;98:181–6.

[19] Madsen BL, His A, Pham HT, et al. Intrafractional stability of the prostate using a stereotactic radiotherapy technique. Int J Radiat Oncol Biol Phys 2003;57:1285–91.

[20] McNair HA, Wedlake L, McVey GP, Thomas K, Andreyev J, Dearnaley DP. Can diet combined with treatment scheduling achieve consistency of rectal filling in patients receiving radiotherapy to the prostate? Radiother Oncol 2011;101:471–8.

[21] Ten Haken RK, Forman JD, Heimberger DK, et al. Treatment planning issues related to prostate movement in response to differential filling of the rectum and bladder. Int J Radiat Oncol Biol Phys 1991;20:1317–24.

[22] Padhani AR, Khoo VS, Suckling J, Husband JE, Leach MO, Dearnaley DP. Evaluating the effect of rectal distension and rectal movement on prostate gland position using cine MRI. Int J Radiat Oncol Biol Phys 1999;44:525–33.

[23] Both S, Wang KK, Plastaras JP, et al. Real-time study of prostate intrafraction motion during external beam radiotherapy with daily endorectal balloon. Int J Radiat Oncol Biol Phys 2011;81:1302–9.

[24] Nichol AM, Warde PR, Lockwood GA, et al. A cinematic magnetic resonance imaging study of milk of magnesia laxative and an antiflatulation diet to reduce intrafractional prostate motion. Int J Radiat Oncol Biol Phys 2010;77:1072–8.

[25] Ghilezan MJ, Jaffray DA, Siewerdsen JH, et al. Prostate gland motion assessed with cine-magnetic resonance imaging (cine-MRI). Int J Radiat Oncol Biol Phys 2005;62:406–17.

[26] Mah D, Freedman G, Milestone B, et al. Measurement of intrafractional prostate motion using magnetic resonance imaging. Int J Radiat Oncol Biol Phys 2002;54:568–75.

[27] Chen L, Paskalev K, Xu X, et al. Rectal dose variation during the course of image-guided radiation therapy of prostate cancer. Radiother Oncol 2010;95:198–202.

[28] Engels B, Tournel K, Soete G, Storme G. Assessment of rectal distention in radiotherapy of prostate cancer using daily megavoltage CT image guidance. Radiother Oncol 2009;90:377–81.

[29] Sripadam R, Stratford J, Henry AM, Jackson A, Moore CJ, Price P. Rectal motion can reduce CTV coverage and increase rectal dose during prostate radiotherapy: a daily cone-beam CT study. Radiother Oncol 2009;90:312–7.

[30] Kron T, Thomas J, Fox C, et al. Intra-fraction prostate displacement in radiotherapy estimated from pre-and post-treatment imaging of patients with implanted fiducial markers. Radiother Oncol 2010;95:191–7.

[31] Xie Y, Djajaputra D, King CR, Hossain S, Ma L, Xing L. Intrafractional motion of the prostate during hypofractionated radiotherapy. Int J Radiat Oncol Biol Phys 2008;72:236–46.

[32] Kitamura K, Shirato H, Seppenwoolde Y, et al. Three-dimensional intrafractional movement of prostate measured during real-time tumor-tracking radiotherapy in supine and prone treatment positions. Int J Radiat Oncol Biol Phys 2002;53:1117–23.

[33] Li JS, Jin L, Pollack A, Horwitz EM, Buyyounouski MK, Price Jr RA, et al. Gains from real-time tracking of prostate motion during external beam radiotherapy. Int J Radiat Oncol Biol Phys 2009;75:1613–20.

[34] Mikuma N, Tamagawa M, Morita K, Tsukamoto T. Magnetic resonance imaging of the male pelvic floor: the anatomical configuration and dynamic movement in healthy men. Neurourol Urodyn 1998;17:591–7.

[35] Christensen LL, Djurhuus JC, Constantinou CE. Imaging of pelvic floor contractions using MRI. Neurourol Urodyn 1995;14:209–16.

Original Article

Extended Field Stereotactic Radiosurgery for Recurrent Glioblastoma

Tomoyuki Koga, MD[1]; Keisuke Maruyama, MD, PhD[1]; Minoru Tanaka, MD, PhD[1]; Yasushi Ino, MD, PhD[1,2]; Nobuhito Saito, MD, PhD[1]; Keiichi Nakagawa, MD, PhD[3]; Junji Shibahara, MD, PhD[4]; and Tomoki Todo, MD, PhD[1,2]

BACKGROUND: Stereotactic radiosurgery (SRS) is among the few therapeutic options for glioblastoma that recurs after standard radiation and chemotherapy, but its efficacy has been limited. **METHODS:** Since November 2007, the authors have modified the clinical target volume by adding a 0.5- to 1-cm margin to the gadolinium-enhanced area (extended field SRS), in contrast to conventional SRS using no margin to set the clinical target volume. A total of 35 recurred glioblastoma lesions in 9 patients were treated with conventional SRS between December 1990 and January 2007, and 14 lesions in 9 patients were treated with extended field SRS. **RESULTS:** The median follow-up periods were 7 months (range, 3-29 months) and 8 months (range, 6-27 months), respectively. The local control rate was 47% for conventional SRS and 93% for extended field SRS ($P = .0035$), and the numbers of radiation necrosis observed in SRS-treated lesions were 2 and 4, respectively. The median overall survival from the diagnosis was 24 months (range, 14-57 months) for conventional SRS and 21 months (range, 15-51 months) for extended field SRS (statistically not significant). Seven patients treated with conventional SRS died during follow-up, 6 from progression of the SRS-treated tumor, whereas 7 patients treated with extended field SRS died during follow-up, 6 from remote intracerebral dissemination. **CONCLUSIONS:** Extended field SRS was superior to conventional SRS in the local control of small recurrent lesions of glioblastoma, although a further device to suppress remote dissemination may be necessary to increase survival. ***Cancer* 2011;000:000–000.** © *2011 American Cancer Society.*

KEYWORDS: glioblastoma, glioma, gamma knife, stereotactic radiosurgery, radiation therapy, recurrence.

INTRODUCTION

Glioblastoma is a highly malignant and aggressive tumor of the central nervous system that corresponds to grade IV of the World Health Organization histological classification.[1] The current standard treatment for glioblastoma is a maximal resection with functional preservation, followed by radiation and chemotherapy. When temozolomide is used for chemotherapy, the median survival is 14.6 months after initial presentation,[2] and ranges from 5 to 13 months after recurrence.[3,4] Because of the aggressive and invasive nature of the tumor, recurrence is seen in >90% of patients.[5] The most common pattern of recurrence is local regrowth[6]; therefore, successful local control should lead to prolongation of patients' survival. Various local treatment strategies have been attempted, including repeated operations, conformal radiotherapy, brachytherapy, and local chemotherapy.[7]

Although stereotactic radiosurgery (SRS) is an option as salvage treatment for recurrent glioblastoma in clinical settings, the role of SRS is still limited for glioma. SRS is useful in controlling relatively well-demarcated glioma such as ependymoma, pilocytic astrocytoma, and pleomorphic xanthoastrocytoma.[8-13] However, the majority of glioma is infiltrative to brain parenchyma and is difficult to target with SRS. A randomized controlled study proved that there was no benefit in upfront SRS before conventional fractionated radiation therapy for patients with glioblastoma.[14] Several reports indicate the usefulness of adjuvant SRS at recurrence for glioblastoma, median survival time after SRS being 4.6 to 16 months,[15-20] although a randomized study is needed to prove efficacy. The major cause of treatment failure in managing recurrent glioblastoma by SRS is assumed to be that the highly conformal irradiation spares the surrounding tissue, which is presumably infiltrated with viable tumor cells.[21-23] With the intent to cover such tissue surrounding the bulk of tumor as much as possible, we changed the treatment protocol of SRS for recurrent glioblastoma lesions by extending the clinical target volume.[24] We present the early results of this newly applied treatment strategy.

Corresponding author: *Tomoki Todo, MD, PhD, Division of Innovative Cancer Therapy, Institute of Medical Science, University of Tokyo, 4-6-1 Shirokanedai,* Minato-ku, Tokyo 108-8639 Japan; Fax: (011) + 81-3-6409-2147; toudou-nsu@umin.ac.jp

[1]Department of Neurosurgery, University of Tokyo Hospital, Tokyo, Japan; [2]Translational Research Center, University of Tokyo Hospital, Tokyo, Japan; [3]Department of Radiology, University of Tokyo Hospital, Tokyo, Japan; [4]Department of Pathology, University of Tokyo Hospital, Tokyo, Japan

DOI: 10.1002/cncr.27372, **Received:** June 12, 2011; **Revised:** September 19, 2011; **Accepted:** October 24, 2011, **Published online** in Wiley Online Library (wileyonlinelibrary.com)

Table 1. Characteristics of the Patients Who Received Conventional SRS

Case No.	Age, y/Sex	Initial Hx	Initial Tx	Time from Dx to 1st SRS, mo	No. of Lesions	Controlled Lesions	Time to Local Relapse, mo	Last F/U, mo after 1st SRS	Outcome
1	25/M	Glioblastoma	EBRT, ACNU	22	3	1/3	4	4	Lost to F/U
2	40/M	Glioblastoma	EBRT, ACNU	17	1	0/1	9	29	Dead
3	43/M	Glioblastoma	EBRT, ACNU	10	3	0/3	10	16	Dead
4	62/M	AA	EBRT, ACNU	1	1	NA	NA	13	Dead
5	43/M	Glioblastoma	EBRT, ACNU	6	5	3/5	7	8	Lost to F/U
6	59/F	Glioblastoma	EBRT, CE	15	6	1/6	6	7	Dead
7	17/F	Glioblastoma	BNCT, TMZ	14	6	5/6	6	6	Dead
8	64/F	Glioblastoma	EBRT, ACNU	19	1	0/1	1	3	Dead
9	54/M	Glioblastoma	EBRT, TMZ	51	9	6/9	5	6	Dead

Abbreviations: AA, anaplastic astrocytoma; ACNU, nimustine hydrochloride; BNCT, boron neutron capture therapy; CE, carboplatin and etoposide; Dx, diagnosis of glioblastoma; EBRT, external beam radiotherapy; F, female; F/U, follow-up; Hx, histology; M, male; NA, data not available; SRS, stereotactic radiosurgery; TMZ, temozolomide; Tx, treatment.

Table 2. Characteristics of the Patients Who Received Extended Field SRS

Case No.	Age/Sex	Primary Hx	Primary Tx	Time from Dx to 1st SRS, mo	No. of Lesions	Controlled Lesions	Time to Local Relapse, mo	Last F/U, mo after 1st SRS	Outcome
1	53/M	Glioblastoma	EBRT, TMZ	17	1	1/1	—	27	Dead
2	27/M	Glioblastoma	EBRT, TMZ	39	1	0/1	1	12	Dead
3	43/M	AA	EBRT, TMZ	18	1	1/1	—	8	Dead
4	63/M	Glioblastoma	EBRT, TMZ	13	1	1/1	—	10	Dead
5	36/M	DA	EBRT, TMZ	9	3	3/3	—	8	Dead
6	66/F	Glioblastoma	EBRT, TMZ	9	3	3/3	—	6	Dead
7	47/M	Glioblastoma	EBRT, TMZ	12	2	2/2	—	7	Dead
8	58/F	Glioblastoma	EBRT, TMZ	6	1	1/1	—	12	Alive
9	79/F	Glioblastoma	EBRT, TMZ	9	1	1/1	—	8	Alive

Abbreviations: AA, anaplastic astrocytoma; DA, diffuse astrocytoma; Dx, diagnosis of glioblastoma; EBRT, external beam radiotherapy; F, female; F/U, follow-up; Hx, histology; M, male; SRS, stereotactic radiosurgery; TMZ, temozolomide; Tx, treatment.

MATERIALS AND METHODS

Patient Population

Nine patients with recurrent glioblastoma underwent 14 sessions of conventional SRS for 35 lesions using the Leksell Gamma Knife at our institute between December 1990 and January 2007 (Table 1). The median patient age was 43 years (range, 17-64 years). The median Karnofsky Performance Scale score at the first presentation was 90% (range, 80%-90%), and the median Karnofsky Performance Scale score at the time of first SRS for recurrence was 90% (range, 40%-90%). All the patients underwent surgical resection followed by radiation and chemotherapy at the primary onset. Primary lesions were histologically diagnosed as glioblastoma in 8 patients. In 1 patient, the primary lesion was diagnosed as anaplastic astrocytoma, but the recurred lesion was histologically confirmed as glioblastoma after resection. As primary treatment, external beam radiotherapy was applied for 8 patients with the median total dose of 60 grays (Gy; range, 48-80 Gy). Twenty-five of the 35 treated lesions (71%) were within the clinical target volume of the preceding radiotherapy. One patient underwent boron neutron capture therapy. For adjuvant chemotherapy, nimustine hydrochloride was used for 7 patients, carboplatin and etoposide for 1 patient, and temozolomide for 1 patient. The median interval between the time of diagnosis as glioblastoma and the recurrence was 14.5 months (range, 1-51 months).

Nine patients with recurrent glioblastoma underwent 11 sessions of extended field SRS for 14 lesions from November 2007 to April 2010 (Table 2). The extended field SRS was applied to a single recurrent lesion or 2 separate lesions that were $\leq$20 mm in diameter. The median age of this patient group was 53 years (range, 27-79 years). The median Karnofsky Performance Scale score at the first presentation was 90% (range, 80%-90%), and the median Karnofsky Performance Scale score at the time of first SRS for recurrence was 70% (range, 40%-90%).

Seven of these 9 patients underwent surgical resection, and 2 patients received stereotactic biopsy. The initial histological diagnosis was glioblastoma in 7 patients, anaplastic astrocytoma in 1 patient, and diffuse astrocytoma in 1 patient. In the latter 2 patients, lesions were histologically confirmed as glioblastoma at the time of recurrence. All of the 9 patients underwent external beam radiation therapy, with the median total dose of 70 Gy (range, 60-80 Gy). Ten of 14 treated lesions (71%) were within the clinical target volume of the preceding radiotherapy. Seven of them were treated with concomitant and adjuvant temozolomide therapy until the time of SRS for recurrences. For 1 patient, temozolomide was discontinued at the third cycle and nimustine hydrochloride administration was started, because of eruption and thrombocytopenia caused by temozolomide. The other patient received nimustine hydrochloride during radiation, and adjuvant temozolomide therapy was applied for up to 21 cycles until he denied the continuation of the chemotherapy. The median interval between the time of diagnosis as glioblastoma and the recurrence was 12 months (range, 6-39 months).

Conventional SRS

After their heads had been immobilized in the Leksell stereotactic head frame, the patients underwent stereotactic magnetic resonance imaging (MRI) to obtain precise information on the shape, volume, and 3-dimensional coordinates of the tumors. Image-integrated treatment planning was performed jointly by neurosurgeons and radiation oncologists with commercially available software (Leksell GammaPlan; Elekta Instruments AB, Stockholm, Sweden). The clinical target volume was defined as the gadolinium-enhanced lesion without any margin. In principle, the desired dose applied to the margin of each gadolinium-enhanced lesion was 20 Gy. The prescription dose was occasionally reduced because of the tumor volume, the location of lesions, and/or the clinical status of the patient. The median clinical target volume of conventional SRS was 15 cm^3 (range, 3-47 cm^3).

Extended Field SRS

The methods of head fixation, obtaining stereotactic images, and treatment planning and the principle for dose prescription were the same as conventional SRS. The difference was the definition of the clinical target volume, which was extended by adding a 0.5- to 1-cm margin to the periphery of the gadolinium-enhanced lesion. Margin was extended up to a maximum of 1 cm in all directions. By using a dose-volume histogram, the volume that received >20 Gy was determined not to exceed 15 cm^3. The clinical target volume exceeded 15 cm^3 in 2 cases, but the lesions in these patients faced the resection cavity or the ventricle, so the volume of the brain parenchyma included in the clinical target volume was <15 cm^3 in both cases. The median clinical target volume of extended field SRS was 13 cm^3 (range, 6-19 cm^3).

Patient Follow-Up and Statistical Analysis

After SRS, follow-up clinical examinations were performed at our hospital or elsewhere by referring physicians. MRI or computed tomography scanning was taken at 1- to 3-month intervals. When a contrast-enhanced lesion continued to grow at follow-up examinations, it was defined as local control failure unless it was histologically confirmed as radiation necrosis. Conversely, if a contrast-enhanced area ceased to expand or decreased in size during the follow-up with or without the use of steroids, the lesion was recognized as radiation necrosis. Statistical analyses were performed using JMP 8 (SAS Institute, Cary, NC). Fisher exact test was performed to evaluate the significance of differences between conventional SRS and extended field SRS regarding the local control rate and the incidence of radiation necrosis, and the correlation between radiation necrosis and the location of treated lesions. The progression-free and overall survival times were calculated using the Kaplan-Meier method. Factors potentially affecting the survival time were evaluated by log-rank test for univariate analysis.

Ethical Issues

The conduct of this study was approved by our institutional review board. All patients provided written informed consent.

RESULTS

Outcomes of Conventional SRS

Characteristics and outcomes of the patients who underwent conventional SRS are summarized in Table 1. Nine patients who underwent SRS targeting gadolinium-enhanced lesions were followed for the median period of 7 months (range, 3-29 months). Among 34 lesions that could be radiographically followed up, 16 lesions (47%) showed <25% increase of the target area or decreased in size in response to SRS until the last follow-up. All patients who died after conventional SRS possessed uncontrolled SRS-treated lesions. The median time to local relapse after SRS was 6 months (range, 1-10 months). The median survival time after the first SRS for recurrences was 10.5 months (range, 3-29 months). The median overall survival time after the diagnosis of glioblastoma was 24 months (range, 14-57 months), and the

6-month overall survival rate was 63%. As for SRS-induced adverse effects, asymptomatic, radiographically confirmed radiation necrosis was observed in 2 lesions in 2 patients (6.5%). Among these 2 lesions, 1 lesion occurred within the clinical target volume of prior radiotherapy and 1 outside ($P = .59$).

Outcomes of Extended Field SRS

Characteristics and outcomes of the patients who underwent extended field SRS are summarized in Table 2. Nine patients who underwent extended field SRS were followed for the median period of 8 months (range, 5-27 months). Thirteen among 14 lesions (93%) showed <25% increase of the target area or decreased in size in response to SRS until the last follow-up. This local control rate was significantly higher than that of conventional SRS ($P = .0035$). The local relapse in the 1 patient (case 2 in Table 2) was histologically confirmed. Whereas the lesions treated by SRS in 8 patients were controlled until the last follow-up, remote recurrences were observed in 5 patients. Two patients (cases 5 and 6 in Table 2) underwent second SRS for those remote lesions. Another patient (case 3 in Table 2) showed a remote recurrence in the brainstem, for which external beam radiotherapy was performed. The median survival time after the first SRS for recurrences was 9 months (range, 6-27 months), and the 6-month overall survival rate was 89%. There was no statistical difference in survival time after SRS between conventional and extended field SRS ($P = .83$). The median overall survival time after the diagnosis of glioblastoma was 21 months (range, 15-51 months), not statistically different from conventional SRS ($P = .71$). Radiation necrosis was observed in 4 lesions in 4 patients (29%), age ranging from 27 to 53 years, and the frequency was not significantly different from conventional SRS ($P = .052$). The irradiated fields for SRS in these 4 patients all involved the irradiated fields of prior radiotherapy, although this was not statistically significant ($P = .25$). All 4 patients required oral administration of prednisolone at doses of 20 to 30 mg (median, 30 mg) for 7 to 25 months (median, 9 months). As for steroid-related toxicities, moon face and central obesity were observed in all 4 patients, and 1 patient experienced urinary tract infection. By the use of oral steroids, radiation necroses became stable and did not cause deterioration of neurological symptoms in any patients. Karnofsky Performance Scale scores of these 4 patients at the time of first SRS were 90%, 70%, 40%, and 70%. Karnofsky Performance Scale score gradually declined in all 4 patients, mainly because of disseminated lesions, and became 70%, 60%, 40%, and 40% at 6 months after first SRS. The 4 patients died of tumor progression at 27, 12, 8, and 14 months after first SRS. Comparison of patient characteristics and treatment outcomes between conventional and extended field SRS is summarized in Table 3.

Table 3. Comparison of Characteristics and Outcomes of the Patients Who Received Conventional SRS and Extended Field SRS

Characteristic	Conventional SRS	Extended Field SRS	*P*
Number of patients	9	9	—
Primary glioblastoma	8	7	1.0
Patient age, median y, range	43, 17-64	53, 27-79	.36
KPS at onset, median, range	90, 80-90	90, 80-90	.62
Time from Dx to 1st SRS, median mo, range	14.5, 1-51	12, 6-39	.66
KPS at 1st SRS, median, range	90, 40-90	70, 40-90	.21
Local control	16/34	13/14	.0035
Radiation necrosis	2/34	4/14	.052
Median OS after Dx, mo	24	21	.71
Median OS after 1st SRS, mo	10.5	9	.83
6-month OS after 1st SRS, %	63	89	.83

Abbreviations: Dx, diagnosis of glioblastoma; KPS, Karnofsky Performance Scale; OS, overall survival; SRS, stereotactic radiosurgery.

Illustrative Cases

A 17-year-old girl (case 7 in Table 1) presented with right hemiparesis. MRI showed a heterogeneously enhanced mass lesion in the left frontal lobe (Fig. 1A). The tumor was subtotally removed and histologically diagnosed as glioblastoma. Boron neutron capture therapy was performed, and temozolomide was administered orally at a dose of 200 mg/m^2 using the 5 of 28-day regimen. Twelve months after the onset, a diffuse recurrence was observed in the left frontal lobe and the corpus callosum, so she received 50-Gy external beam radiotherapy in 25 fractions. At 14 months, a recurrent lesion 7 mm in diameter was noted in the right frontal lobe, and it was treated by conventional SRS targeting the gadolinium-enhanced lesion with a maximum dose of 40 Gy and a margin dose of 20 Gy (Fig. 1B). However, this lesion continued to grow at 1 month (Fig. 1C) and 3 months (Fig. 1D) after the SRS, and the patient died of diffuse dissemination at 3 months after the SRS.

A 53-year-old man (case 1 in Table 2) presented with left hemiparesis. MRI showed a homogeneously enhanced, poorly circumscribed mass lesion in the right frontal lobe (Fig. 2A). The tumor was subtotally removed and histologically diagnosed as glioblastoma. He received 80-Gy external beam radiotherapy in 40 fractions, with

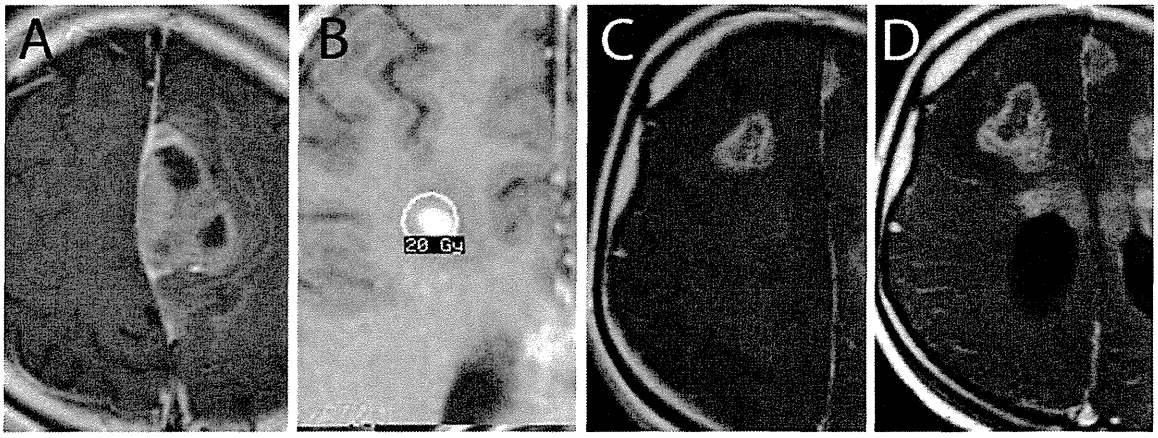

Figure 1. Case 7 in Table 1 is shown: (A) axial gadolinium-enhanced T1-weighted magnetic resonance imaging (MRI) at presentation; (B) dose planning of stereotactic radiosurgery for recurrence; (C, D) MRI taken at 1 (C) and 3 months (D) after stereotactic radiosurgery showing tumor progression.

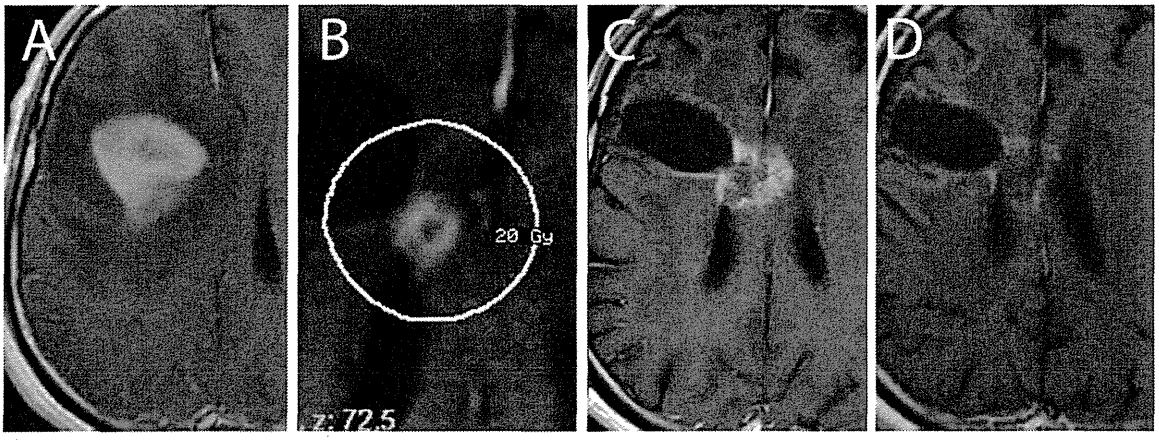

Figure 2. Case 1 in Table 2 is shown: (A) axial gadolinium-enhanced T1-weighted magnetic resonance imaging (MRI) at presentation; (B) dose planning of stereotactic radiosurgery for recurrence; (C) MRI taken at 1 month after stereotactic radiosurgery showing diffuse enhancement around treated lesion; (D) MRI taken at 25 months after stereotactic radiosurgery showing no recurrence.

which temozolomide at a dose of 200 mg/m^2 using the 5 of 28-day regimen was initiated. After the third cycle of temozolomide, eruption and thrombocytopenia were observed, so chemotherapy was switched to nimustine hydrochloride (100 mg/dose), which was administered intravenously once a month thereafter. Although complete remission was maintained until 17 months after the onset, a recurrent lesion 10 mm in diameter was observed near the resection cavity in the right frontal lobe. Extended field SRS was applied to this lesion. The clinical target volume was set as the gadolinium-enhanced lesion plus a 1-cm–wide margin, and 20 Gy was prescribed at the margin of this wide target (Fig. 2B). One month after the SRS, diffuse enhancement around the irradiated area was observed (Fig. 2C). As radiation necrosis was suspected, oral prednisolone at a dose of 30 mg daily was initiated, and the area of enhancement ceased to expand thereafter. At 25-month follow-up after the SRS, the treated lesion had been locally controlled, and no new recurrence was noted (Fig. 2D).

A 27-year-old man (case 2 in Table 2) presented with right hemiparesis. MRI revealed a homogeneously enhanced mass in the right frontal lobe (Fig. 3A). Stereotactic biopsy was performed, and the diagnosis of glioblastoma was obtained. He received 60-Gy external beam radiotherapy followed by adjuvant temozolomide at a dose of 200 mg/m^2 using the 5 of 28-day regimen. Complete remission was achieved and maintained until 39 months after the onset, when a recurrent lesion (maximal diameter, 15 mm) was noted in the right frontal lobe

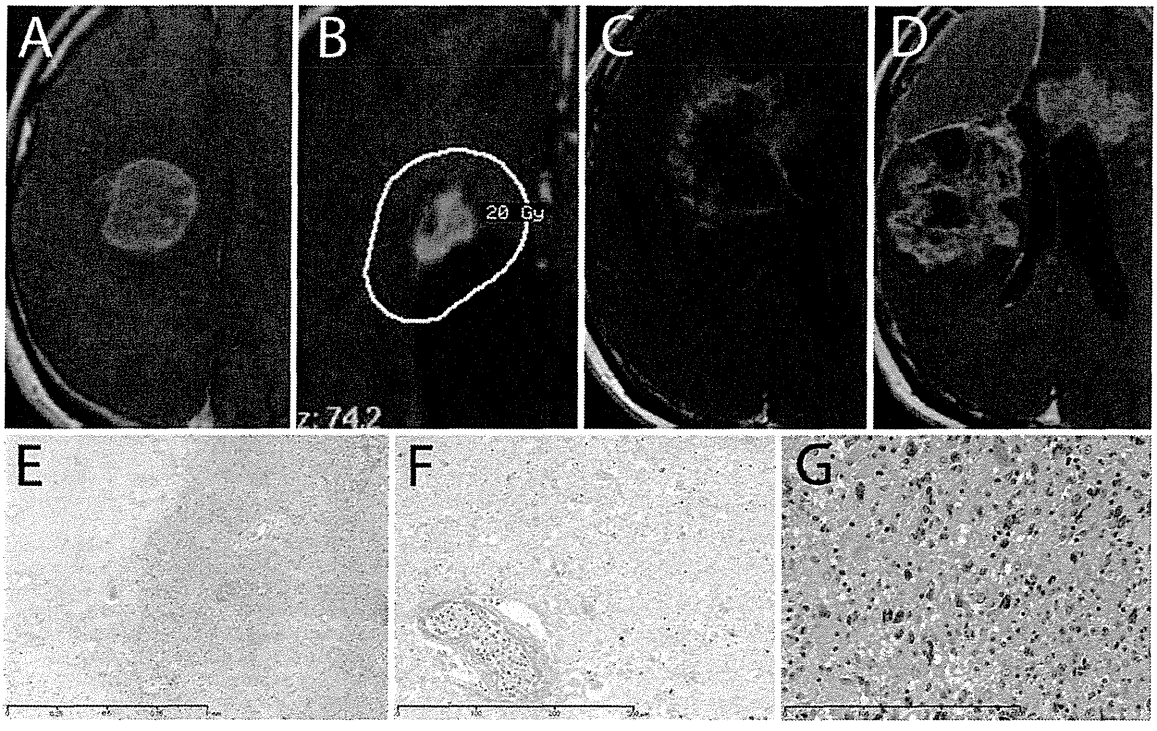

Figure 3. Case 2 in Table 2 is shown. (A) Axial gadolinium-enhanced T1-weighted magnetic resonance imaging (MRI) at presentation is shown. (B) Dose planning of stereotactic radiosurgery for recurrence. (C) MRI taken at 5 month after stereotactic radiosurgery revealed progression of enhancing lesion around the treated area. (D) MRI taken at 12 months after stereotactic surgery revealed continued tumor growth. (E-G) Hematoxylin and eosin staining of a surgical specimen at recurrence (E) revealed focuses of radiation necrosis (F) surrounded by an area of tumor with high cellularity (G).

beneath the wall of the right lateral ventricle. This recurred lesion was treated by extended field SRS targeting the gadolinium-enhanced lesion plus a 1-cm–wide margin. Prescribed margin dose was 20 Gy (Fig. 3B). Heterogeneous enhancement appeared at the irradiated site 1 month after the SRS and continued to grow despite the use of oral prednisolone. Frontal lobectomy was performed 5 months after the SRS to decrease the tumor mass that caused deterioration of the consciousness level (Fig. 3C). Recurrence of glioblastoma was confirmed by a histological examination, and the tumor continued to grow diffusely after the surgery. The patient died of tumor progression 12 months after the SRS for recurrence (Fig. 3D). Histologically, the surgical specimens at recurrence (Fig. 3E) consisted of focal areas of radiation necrosis (Fig. 3F) surrounded by areas of viable tumors with high cellularity consistent with glioblastoma (Fig. 3G).

DISCUSSION

Our results showed that extended field SRS potentially provided improved local control of isolated recurrence of glioblastoma without causing uncontrollable symptomatic radiation necrosis. In several studies analyzing patients treated with radiation and temozolomide, 72% to 92% of recurrence was revealed as local relapse,[25,26] the most frequent pattern of glioblastoma recurrence.[6] Local control is also important for recurrent lesions, but treatment with SRS led to local progression in 65% to 90%,[14,27-29] which was in line with our result with conventional SRS targeting only the gadolinium-enhanced area. The logical assumption regarding the reason for this lack of efficacy is that SRS, owing to its characteristic feature of steep dose falloff, is unable to kill tumor cells infiltrating the tissue outside the irradiated field.[20,27] When we extended the irradiation field with the intent to include as many tumor cells invasive to the surrounding tissue as possible, we achieved a high local control rate of 93%. This result showed that extended field SRS was highly effective in controlling recurrent glioblastoma for selected patients found with small lesions. One limitation of this treatment is that it is not applicable to lesions larger than approximately 20 mm in diameter. Adding a sufficient margin to a large lesion results in a large prescribed isodose volume, and may cause uncontrollable radiation-

induced adverse events. A close radiological follow-up after the initial treatment is necessary to detect such small recurrent lesions for this treatment to be suitable for an extended field SRS application. Stereotactic fractionated radiotherapy may be 1 treatment option for larger recurrent lesions. By using 11-C-methionine positron emission tomography for targeting, stereotactic fractionated radiotherapy was reported to have achieved the median survival time of 9 months.[30] Although the incidence of radiation necrosis after SRS was not significantly different between conventional and extended field SRS, all patients who developed radiation necrosis after extended field SRS required steroid administration. This risk of eventual necessity of steroid administration may be another limitation of this approach.

Whereas extended field SRS achieved a high local tumor control rate, it did not show a significant survival benefit compared with conventional SRS in our study. All patients treated with extended field SRS received external beam radiation therapy and temozolomide before SRS. The majority of patients treated with extended field SRS died of remote recurrences within the brain. Because the rates of new recurrences in patients treated with temozolomide and radiation are quite high to begin with, 25% at 1 year and 66% at 2 years,[26] the role of extended field SRS for the occurrence of remote recurrences is unclear. Obviously, radiation therapy, including SRS, and temozolomide are not sufficient to control the disease. New approaches are underway, including monoclonal antibodies that target specific molecules, for example, bevacizumab,[31,32] and oncolytic viruses that replicate selectively in tumor cells.[33]

In conclusion, extended field SRS was well tolerated and superior to conventional SRS in the local control of small recurrent lesions of glioblastoma, although a further device to suppress remote recurrences may be necessary to improve survival.

FUNDING SOURCES

No specific funding was disclosed.

CONFLICT OF INTEREST DISCLOSURES

The authors made no disclosures.

REFERENCES

1. Louis DN, Ohgaki H, Wiestler OD, Cavenee WK. World Health Organization Histological Classification of Tumours of the Central Nervous System. 4th ed. Lyon, France: International Agency for Research on Cancer; 2007.
2. Stupp R, Mason WP, van den Bent MJ, et al. Radiotherapy plus concomitant and adjuvant temozolomide for glioblastoma. *N Engl J Med.* 2005;352:987-996.
3. Dirks P, Bernstein M, Muller PJ, Tucker WS. The value of reoperation for recurrent glioblastoma. *Can J Surg.* 1993;36:271-275.
4. Larson DA, Suplica JM, Chang SM, et al. Permanent iodine 125 brachytherapy in patients with progressive or recurrent glioblastoma multiforme. *Neuro Oncol.* 2004;6:119-126.
5. Wong ET, Hess KR, Gleason MJ, et al. Outcomes and prognostic factors in recurrent glioma patients enrolled onto phase II clinical trials. *J Clin Oncol.* 1999;17:2572-2578.
6. Chang SM, Parney IF, Huang W, et al. Patterns of care for adults with newly diagnosed malignant glioma. *JAMA.* 2005;293:557-564.
7. Hau P, Baumgart U, Pfeifer K, et al. Salvage therapy in patients with glioblastoma: is there any benefit? *Cancer.* 2003;98:2678-2686.
8. Kano H, Niranjan A, Kondziolka D, Flickinger JC, Lunsford LD. Outcome predictors for intracranial ependymoma radiosurgery. *Neurosurgery.* 2009;64:279-287.
9. Kinoshita M, Izumoto S, Kagawa N, Hashimoto N, Maruno M, Yoshimine T. Long-term control of recurrent anaplastic ependymoma with extracranial metastasis: importance of multiple surgery and stereotactic radiosurgery procedures—case report. *Neurol Med Chir (Tokyo).* 2004;44:669-673.
10. Endo H, Kumabe T, Jokura H, Shirane R, Tominaga T. Stereotactic radiosurgery for nodular dissemination of anaplastic ependymoma. *Acta Neurochir (Wien).* 2004;146:291-298.
11. Kano H, Kondziolka D, Niranjan A, Flickinger JC, Lunsford LD. Stereotactic radiosurgery for pilocytic astrocytomas part 1: outcomes in adult patients. *J Neurooncol.* 2009;95:211-218.
12. Koga T, Morita A, Maruyama K, et al. Long-term control of disseminated pleomorphic xanthoastrocytoma with anaplastic features by means of stereotactic irradiation. *Neuro Oncol.* 2009;11:446-451.
13. Larson DA, Gutin PH, McDermott M, et al. Gamma knife for glioma: selection factors and survival. *Int J Radiat Oncol Biol Phys.* 1996;36:1045-1053.
14. Souhami L, Seiferheld W, Brachman D, et al. Randomized comparison of stereotactic radiosurgery followed by conventional radiotherapy with carmustine to conventional radiotherapy with carmustine for patients with glioblastoma multiforme: report of Radiation Therapy Oncology Group 93-05 protocol. *Int J Radiat Oncol Biol Phys.* 2004;60:853-860.
15. Kondziolka D, Flickinger JC, Bissonette DJ, Bozik M, Lunsford LD. Survival benefit of stereotactic radiosurgery for patients with malignant glial neoplasms. *Neurosurgery.* 1997;41:776-783.
16. Chamberlain MC, Barba D, Kormanik P, Shea WM. Stereotactic radiosurgery for recurrent gliomas. *Cancer.* 1994;74:1342-1347.
17. Kong DS, Lee JI, Park K, Kim JH, Lim DH, Nam DH. Efficacy of stereotactic radiosurgery as a salvage treatment for recurrent malignant gliomas. *Cancer.* 2008;112:2046-2051.
18. Combs SE, Widmer V, Thilmann C, Hof H, Debus J, Schulz-Ertner D. Stereotactic radiosurgery (SRS): treatment option for recurrent glioblastoma multiforme (GBM). *Cancer.* 2005;104:2168-2173.
19. Mehta MP, Masciopinto J, Rozental J, et al. Stereotactic radiosurgery for glioblastoma multiforme: report of a prospective study evaluating prognostic factors and analyzing long-term survival advantage. *Int J Radiat Oncol Biol Phys.* 1994;30:541-549.
20. Masciopinto JE, Levin AB, Mehta MP, Rhode BS. Stereotactic radiosurgery for glioblastoma: a final report of 31 patients. *J Neurosurg.* 1995;82:530-535.
21. Wallner KE, Galicich JH, Krol G, Arbit E, Malkin MG. Patterns of failure following treatment for glioblastoma multiforme and anaplastic astrocytoma. *Int J Radiat Oncol Biol Phys.* 1989;16:1405-1409.
22. Hochberg FH, Pruitt A. Assumptions in the radiotherapy of glioblastoma. *Neurology.* 1980;30:907-911.
23. Massager N, Maris C, Nissim O, Devriendt D, Salmon I, Levivier M. Experimental analysis of radiation dose distribution in radiosurgery. II. Dose fall-off outside the target volume. *Stereotact Funct Neurosurg.* 2009;87:137-142.
24. Schiffer D, Cavalla P, Dutto A, Borsotti L. Cell proliferation and invasion in malignant gliomas. *Anticancer Res.* 1997;17:61-69.
25. Brandes AA, Tosoni A, Franceschi E, et al. Recurrence pattern after temozolomide concomitant with and adjuvant to radiotherapy in